Atmósfera 39, 77-105 (2025)
https://doi.org/10.20937/ATM.53408

Air quality in the Metropolitan Zone of the Valley of Puebla: Comparative evaluation of CAMS and persistence forecasts

Javier Omar CASTILLO-MIRANDA[1]*, José Carlos MENDOZA-HERNÁNDEZ[1], José Agustín GARCÍA-REYNOSO[2] and Gabriela PÉREZ-OSORIO[1]

[1] *Facultad de Ingeniería Química, Benemérita Universidad Autónoma de Puebla, Calle 4 Sur 104, Colonia Centro, C.P. 72000, Puebla, México.*
[2] *Instituto de Ciencias de la Atmósfera y Cambio Climático, Universidad Nacional Autónoma de México, Circuito de la Investigación Científica, Ciudad Universitaria, C.P. 04510, Ciudad de México, México.*
*Corresponding author; email: j9lechatelier@yahoo.com.mx

Received: June 29, 2024; Accepted: October 18, 2024

RESUMEN

El contexto de la calidad del aire en la Zona Metropolitana del Valle de Puebla muestra que las partículas suspendidas menores de 10 micrómetros (PM_{10}) y de 2.5 micrómetros ($PM_{2.5}$) representan un riesgo para la salud. El sistema automático de monitoreo de la calidad del aire de Puebla mide PM_{10} y $PM_{2.5}$ en cinco estaciones ubicadas en los municipios de Puebla y Coronango. Estas mediciones permiten determinar el Índice de Calidad del Aire y Salud conforme a la norma NOM-172-SEMARNAT-2019 para estos contaminantes. El avance de las técnicas globales de modelado de contaminantes representa una oportunidad para la gestión de la calidad del aire en áreas con escasas mediciones terrestres. Sin embargo, es necesario validar los pronósticos globales con mediciones en tierra provenientes de estaciones de monitoreo georreferenciadas para reducir incertidumbres y determinar su confiabilidad. El pronóstico del Servicio de Monitoreo Atmosférico Copernicus (CAMS) permite explorar los procesos de contaminación atmosférica en la región de estudio. Este estudio presenta un análisis del pronóstico de CAMS frente al pronóstico por persistencia. Los resultados muestran que éste tiene un mejor desempeño en general que el de CAMS, tanto para PM_{10} como para $PM_{2.5}$. Sin embargo, el uso del pronóstico de CAMS es factible para una evaluación preliminar de la predicción de $PM_{2.5}$ debido a sus valores aceptables en los criterios de comparación de las estadísticas dicotómicas ACCURACY, probabilidad de detección (POD), tasa de falsas alarmas (FAR), probabilidad de detección falsa (POFD), índice de éxito (SR), puntaje de amenaza (TS), puntaje de amenaza equitativo (ETS), puntaje de habilidad de Heidke (HSS) y puntaje de habilidad de razón de probabilidades (ORSS). Este trabajo proporciona información valiosa tanto para la población como para los responsables de la toma de decisiones, contribuyendo a mejorar la gestión de la calidad del aire y las estrategias de salud pública.

ABSTRACT

Background on air quality in the Metropolitan Zone of the Valley of Puebla shows that suspended particles smaller than 10 micrometers (PM_{10}) and smaller than 2.5 micrometers ($PM_{2.5}$) represent a health risk. Puebla's automatic air quality monitoring system measures PM_{10} and $PM_{2.5}$ at five stations in the municipalities of Puebla and Coronango. These measurements allow for determining the Air and Health Index according to the NOM-172-SEMARNAT-2019 standard for these pollutants. The advancement of global pollutant modeling techniques represents an opportunity for air quality management in areas with scarce terrestrial measurements. However, it is necessary to validate global forecasts with ground measurements from georeferenced monitoring stations to reduce uncertainties and determine reliability. The Copernicus Atmospheric Monitoring Service (CAMS) forecast allows atmospheric pollution exploration processes in the study region. This study presents an analysis of the CAMS forecast against the Persistence forecast. The results show that the persistence forecast performs better than the CAMS forecast in general, both for PM_{10} and for $PM_{2.5}$. However, using the CAMS forecast for a preliminary evaluation of the prediction of $PM_{2.5}$ is feasible due to its acceptable values in the comparison criteria of the dichotomous statistics ACCURACY, probability of detection (POD), false alarm rate (FAR), probability of false detection (POFD), success ratio (SR), threat score (TS), equitable threat score (ETS), Heidke skill score (HSS), and odds ratio skill score (ORSS). This work provides valuable insights to both the population and decision-makers, aiding in the enhancement of air quality management and public health strategies.

Keywords: $PM_{2.5}$ and PM_{10} air quality, CAMS, contingency tables, dichotomous statistics, satellite monitoring.

1. Introduction

The Clean Air Institute (CAI) study emphasizes the need for environmental improvements in Latin American cities through public policies, highlighting Brazil and Mexico as the countries with the highest number of premature deaths due to air pollution in 2008 (Green and Sánchez, 2013). An estimate of exposure to fine suspended particles in 2019 revealed that they caused 4.2 million premature deaths in cities and rural areas worldwide (WHO, 2024). In addition, 380 000 premature deaths have been associated with air pollution in the Americas this year (PAHO, 2024).

In 2011, 64% of asthma-related deaths in Mexico occurred in children under five, with states like Veracruz and Chiapas most affected. The OECD warns that air pollution could become the leading cause of premature death globally if trends continue (REDIM, 2013).

A study in the State of Puebla considers it highly likely that the following morbidity and mortality risks are linked to air pollution: About morbidity, 1 229 585 cases of acute respiratory infections and 13412 cases of arterial hypertension stand out. Regarding mortality, 8251 cases of heart disease, 2004 of cerebrovascular diseases, 1418 of influenza and pneumonia, 1299 of chronic obstructive pulmonary diseases, and 219 of emphysema and asthma were recorded (SMADSOT, 2023a).

Globally, ambient air pollution and $PM_{2.5}$ are significant health risks, contributing to millions of deaths annually (Cohen et al., 2017). Studies link air pollution to cardiovascular and respiratory diseases, with increases in PM concentration correlating with higher mortality rates (MacNee and Donalson, 2000; Samet et al., 2000; Pope et al., 2004; SEDEMA, 2020). Satellite remote sensing offers new opportunities for air pollution monitoring, enabling broader geographic coverage (Hollingsworth et al., 2008), and models show that $PM_{2.5}$ exposure increases mortality by 2.8% per 10 $\mu g\ m^{-3}$ rise (Kloog et al., 2013).

Ninety-five percent of the global population lives in areas exceeding WHO's $PM_{2.5}$ guidelines (WHO, 2006; Shaddick, 2018). Despite a 46% decrease in the mortality rate due to air pollution, deaths caused by suspended particles increased by 93% in 1990-2021. This places them in a second level of lethality regarding health on the planet (IHME, 2024).

European initiatives like the Copernicus Programme and the Copernicus Atmospheric Monitoring Service (CAMS) use satellite data to forecast air quality and monitor atmospheric conditions (Hollingsworth et al., 2008; Eskes et al., 2015; Wagner et al., 2015). Data assimilation techniques improve model accuracy by combining satellite and ground-based data (Benedetti et al., 2009; Morcrette et al., 2009; Flemming et al., 2013), and regional models in Europe contribute to urban-level air quality predictions (Granier et al., 2011; Kukkonen et al., 2012).

In China, satellite data has been integrated to analyze $PM_{2.5}$ concentrations and their influencing factors (Zhang et al., 2020). CAMS forecasts of $PM_{2.5}$ and PM_{10} have been found to underestimate concentrations during winter (Pappa and Kioutsioukis, 2021). India's Air Quality Early Warning System (AQEWS) effectively uses satellite and ground data to represent PM_{10} variability (Kalita et al., 2023).

1.1 Study area

The study area covers the Metropolitan Zone of the Valley of Puebla (MZVP) in central Mexico, specifically the municipality of Puebla, which has a population of 1 576 259 and spans 524.31 km² (INEGI, 2017). The MZVP is approximately 130 km southeast of Mexico City. Air quality challenges stem mainly from the rising number of vehicles, unregulated urban expansion, and limited emissions regulations.

Since 2000, the vehicle fleet has grown by 89.2%, increasing congestion and pollution (PMD, 2021). Forest degradation, driven by illegal logging and urban expansion, has also worsened environmental conditions, with 25.2% of forested areas damaged between 1984 and 2018 (INEGI, 2018). Additionally, the region's temperate subhumid climate, influenced by wind patterns and the nearby La Malinche volcano, affects pollutant dispersion. The rainy season runs from May to October, with an average annual temperature of 18 °C in the municipality's southern areas (PMD, 2011).

1.2 Air pollution in the Metropolitan Zone of the Valley of Puebla

Air pollution in the MZVP is monitored by the Red Estatal de Monitoreo Atmosférico (State Ambient Air Monitoring Network, REMA), which has been operational since 2000. REMA consists of five continuous monitoring stations that measure pollutants like carbon monoxide, sulfur dioxide, nitrogen dioxide, ozone, PM_{10}, and $PM_{2.5}$, as well as meteorological parameters (INECC, 2019; REMA, 2023). Air quality in the municipality of Puebla frequently exceeds permissible limits, with PM_{10} concentrations surpassing the 24-h limit on 72 days in 2019 and $PM_{2.5}$ showing high concentrations between January and May (INECC, 2020). The Secretaría de Medio Ambiente y Recursos Naturales (Secretariat of Environment and Natural Resources, SEMARNAT) established guidelines for communicating and reporting the Air Quality and Health Risk Index (SEMARNAT, 2019). During the hot-dry season of 2021, PM_{10} levels surpassed the maximum allowable limits on 59 days (SMADSOT, 2021). PM_{10} and $PM_{2.5}$ are formed from natural and human activities, contributing to environmental issues like reduced visibility and nutrient deposition in ecosystems (USEPA, 2020; SEDEMA, 2020).

Air pollution, particularly particulate matter like PM_{10} and $PM_{2.5}$, poses significant health risks in Puebla City, where air quality frequently exceeds the established safety limits. REMA highlights the persistent challenges in maintaining air quality, with pollution levels often surpassing national standards, especially during the hot-dry season. CAMS offers a powerful tool for forecasting air quality, providing valuable data on pollutant concentrations. However, to ensure the accuracy and relevance of these forecasts for local conditions, it is essential to evaluate CAMS predictions compared to simpler persistence forecasts. This comparison will help assess the reliability of CAMS in predicting air quality in Puebla City. This work aims to evaluate CAMS air quality forecasts, compare them with persistence models, and provide actionable insights to the population and decision-makers, supporting better air quality management and public health strategies.

2. Materials and methods

2.1 Methodological scheme

The procedure starts with the Atmospheric Data Store (ADS) platform, the primary data source from CAMS. This system grants access to the global atmospheric composition forecast section of CAMS. The process involves directly discharging the aerosol variables $PM_{2.5}$ and PM_{10} at the surface level. The study period spans from December 31, 2020, to December 31, 2021, with daily downloads scheduled at 00:00 UTC, covering a delivery period of 0 to 23 h.

The methodological process, represented in Figure 1, begins with the weekly download of files in netCDF format in a geographical area defined by the following geographical coordinates with decimal notation: north 19.46, south 18.71, east –97.83 and west –98.71 included in the MZVP (CAMS, 2023).

The procedure continues with the integration of the databases by processing data using a Python script. This script extracts PM_{10} and $PM_{2.5}$ values based on the georeferenced locations of the monitoring network stations using the nearest neighbor method. The original units in kg m^{-3} are converted to µg $m–^{3}$ within the same script.

Subsequently, the databases are generated by calculating the air and health indices (AHI). The AHI calculation procedure with data from the CAMS forecast is described in the standard (SEMARNAT, 2019). Another Python script is used for this, generating 8760 AHI records per station. The CAMS forecast AHI database includes 43 800 records, corresponding to the estimated values for the five stations of the REMA.

The REMA AHI database of PM_{10} and $PM_{2.5}$ comprises the download of the data from the Automatic Air Quality Monitoring Network page corresponding

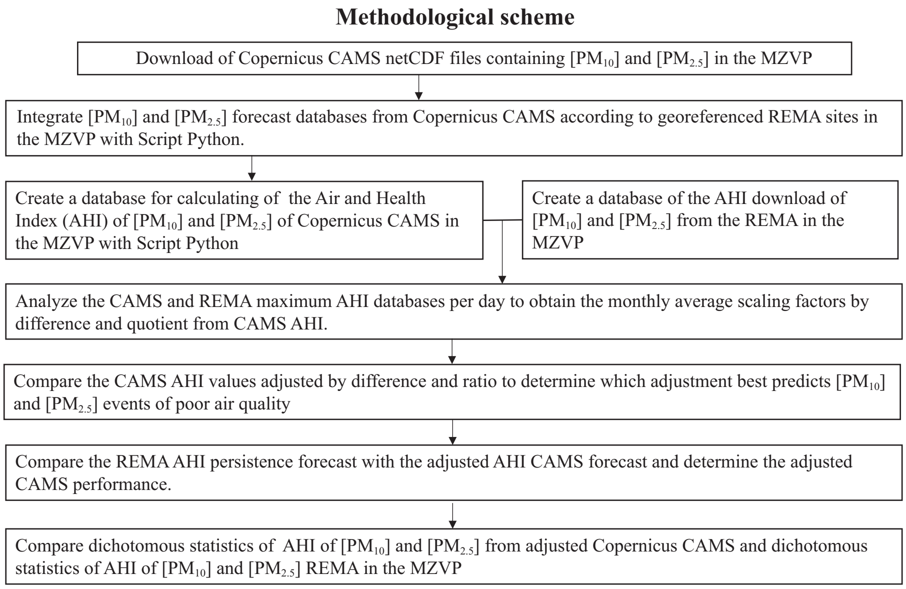

Fig. 1. Methodology for acquiring data, generating contingency tables and deriving results. (Source: self elaboration.)

to 2021 (REMA, 2023). The concentration database for $PM_{2.5}$ integrates 4045 records for the Agua Santa station (STA), 4567 records for the BINE station, 7200 records for the NINFAS station, 6822 records for the UTP station, and no records for the Velódromo station. The concentration database for PM_{10} contains 4680 records for the Agua Santa station (STA), 7622 records for the BINE station, 7758 records for the NINFAS station, 6982 records for the UTP station, and 1135 records for the Velódromo station. Figure 2 represents the geographical location of the stations (SMADSOT, 2023b).

The maximum daily concentrations from the CAMS and REMA databases were used to calculate monthly scale factors. These were derived by two methods: one based on the difference between the measured AHI and the modeled CAMS data and another using the ratio between AHI and CAMS. The $PM_{2.5}$ and PM_{10} concentrations provided by the CAMS forecast are defined within a grid of approximate dimensions of 40 × 40 km, while the station measurements are punctual. This discrepancy introduces a systematic error because the CAMS concentrations obtained at the sites corresponding to the monitoring network stations tend to be underestimated. This error can be reduced using scale factors calculated from the difference or ratio between observed and modeled values. Thus, the CAMS value is adjusted to the REMA AHI results.

The CAMS and REMA databases of maximum daily AHI were analyzed to calculate monthly average scaling factors, using the difference and the ratio between the CAMS AHI and the measured AHI. The procedure involves extracting the maximum daily AHI and CAMS concentration values for each month of the study period. For the difference-based scaling factor, the daily difference between AHI and CAMS is calculated, and a monthly average is derived from these values. This monthly average is added to the daily CAMS concentration to obtain the difference-adjusted CAMS value. In the case of the ratio-based scaling factor, the daily AHI concentration is divided by the CAMS concentration, and the monthly average of these ratios is calculated. This average is multiplied by the daily CAMS AHI to produce the ratio-adjusted CAMS value.

Likewise, comparing the CAMS concentration values adjusted by difference and ratio determines which adjustment best predicts the poor air quality events of PM_{10} and $PM_{2.5}$. These adjusted values are intended to predict the occurrence of events with poor air quality, according to the AHI, which indicates poor air quality when is greater than 45 ($\mu g\ m^{-3}$) for $PM_{2.5}$ and greater than 75 ($\mu g\ m^{-3}$) for PM_{10},

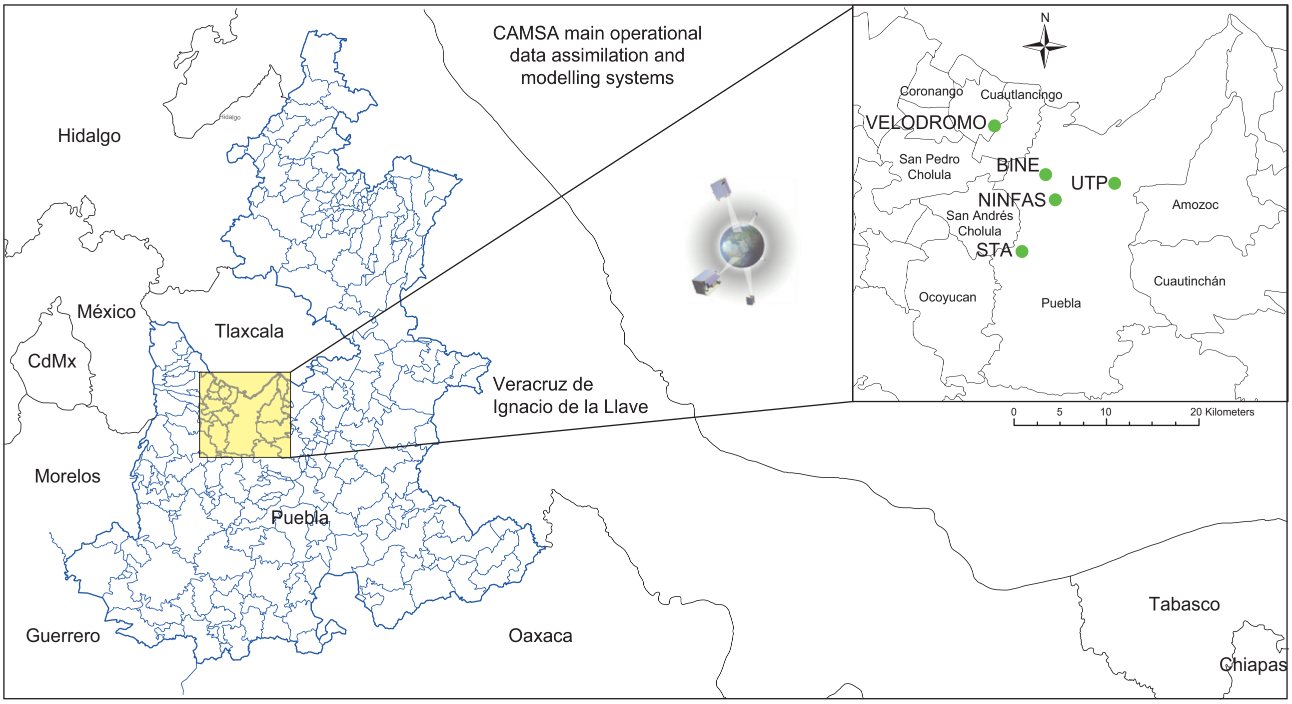

Fig. 2. Location of the monitoring stations in the ZMVP. (ZMVP: Metropolitan Zone of the Valley of Puebla. Source: self elaboration.)

according to the 12-h weighted moving average interval (SEMARNAT, 2019). This procedure allows us to determine which scaling factor provides the best fit to predict poor air quality events at the stations of the atmospheric monitoring network.

Persistence forecasting is a technique used in weather and air quality prediction. It is based on the idea that current atmospheric conditions will continue unchanged. This forecast is used as a reference point to evaluate the accuracy of other more complex forecast models. Comparing the predictions of these models with the persistence forecast can help determine their ability to capture changes in atmospheric conditions and pollution levels.

2.2 Statistical metrics for dichotomous variables

Comparing the REMA AHI persistence forecast with the adjusted CAMS concentration forecast and determining the adjusted CAMS performance is part of the methodological process. However, it is worth mentioning that the persistence forecast serves as a basis for comparison with the CAMS forecast, which allows us to evaluate its performance. We use 2 × 2 contingency tables to categorize days of the year into those that exceed or do not exceed the AHI into three groups of data: measurements, persistence forecast, and CAMS forecast.

Dichotomous statistics classify events into "yes, the event occurs" or "no, the event does not occur". To evaluate this type of classification, 2 × 2 contingency tables are used. These consist of four cells representing the following categories for a persistence forecast: successes (forecasted yes, observed yes), failures (forecasted no, observed no), false alarms (forecasted yes, observed no), and correct negatives (forecasted no, observed no). In the lower right corner of the contingency table are the total counts of observed and predicted events and non-events, as shown in Table I, and are called marginal distribution (WWRP-WGNE, 2017; Gold et al., 2020).

The contingency table is a valuable tool for identifying the types of errors in forecasts. An ideal forecasting method should produce only hits and the correct negatives without presenting failures or false alarms. By combining elements of the contingency table, we can derive dichotomous statistics that

Table I. Contingency table.

		Observed		Total
		Yes	No	
Forecast	Yes	Hits	False alarms	Forecast yes
	No	Misses	Correct negatives	Forecast no
Total		Observed yes	Observed no	Total

provide information on various aspects of forecast performance. Table II shows the optimal values of these dichotomous statistics, described in Gold et al. (2020), where the optimal value is when the values of the model and observations are equal. Descriptions of dichotomous statistical scores can be found in various studies (WWRP-WGNE, 2017).

Table II. Metric, range, and associated optimal values.

Metric	Range	Optimal value
ACCURACY	0 to 1	1
BIAS	0 to ∞	1
POD	0 to 1	1
FAR	0 to 1	0
POFD	0 to 1	0
SR	0 to 1	1
TS	0 to 1	1
ETS	–1/3 to 1	1
HK	–1 to 1	1
HSS	–1 to 1	1
ORSS	–1 to 1	1

ACCURACY: accuracy; POD: probability of detection; FAR: false alarm rate; POFD: probability of false detection; SR: success ratio; TS: threat score; ETS: equitable threat score; HSS: Heidke skill score; ORSS: odds ratio skill score.

2.2 1 CAMS forecast evaluation using AHI based on ground measurements

The comparison of the dichotomous statistics of PM_{10} and $PM_{2.5}$ of adjusted CAMS and dichotomous statistics of PM_{10} and $PM_{2.5}$ REMA in the MZVP is an integral part of the methodological mechanism on which the evaluation method is based.

The dichotomous evaluation uses the concentration databases for $PM_{2.5}$ and PM_{10}, incorporating data from the monitoring network measurements and the CAMS forecast model. The dichotomous verification contemplates the following premise: it evaluates whether the concentration exceeds 45 µg m^{-3} for $PM_{2.5}$ and 75 µg m^{-3} for PM_{10}. This evaluation results in a "yes" or "no", "true" or "false" determination for both the observed and modeled values.

The AHI indicates that air quality is considered poor and presents a high risk when the 12-h weighted moving average exceeds 45 µg m^{-3} for $PM_{2.5}$ and 75 µg m^{-3} for PM_{10}, according to SEMARNAT (2019).

3. Results and discussion

3.1 Comparison of difference and ratio-adjusted CAMS AHI values

Tables III and IV show the monthly average scaling factors by difference and ratio for $PM_{2.5}$ and PM_{10}. These are derived from a comparison between the maximum values per day between CAMS and REMA and are intended to determine which setting best predicts the poor air quality events of PM_{10} and $PM_{2.5}$.

Tables V and VI represent the number of times in a month that $PM_{2.5}$ and PM_{10} exceed the poor air quality level. This is after applying the difference and ratio adjustment. Table V shows that the ratio adjustment for $PM_{2.5}$ significantly increases the number of events where the AHI is greater than 45 µg m^{-3} at the Agua Santa, Ninfas, and UTP stations. The difference adjustment is only greater at the BINE station of the atmospheric monitoring network. Therefore, the ratio adjustment is suitable for predicting $PM_{2.5}$ poor air quality events.

Table VI compares the number of times the AHI for PM_{10} exceeded 75 µg m^{-3} across different monitoring stations in Puebla, using two different adjustment methods: the CAMS adjustment by difference and the CAMS adjustment by ratio.

Table III. Scaling factors by adjustment ratio and average monthly difference of $PM_{2.5}$

Month	Scaling factor by ratio (REMA/CAMS) monthly average of $PM_{2.5}$				Scaling factor by difference (REMA – CAMS) monthly average of $PM_{2.5}$			
	Agua Santa	BINE	Ninfas	UTP	Agua Santa	BINE	Ninfas	UTP
January	0.00	1.58	1.41	1.77	–24.35	1.04	7.64	10.74
February	0.00	1.41	1.77	1.76	–9.80	20.04	7.07	16.67
March	0.00	0.76	1.52	1.73	20.64	9.54	3.01	14.44
April	2.38	1.48	1.12	1.55	22.22	6.76	–0.06	9.40
May	2.05	1.07	0.85	1.52	13.20	–3.09	–6.61	8.61
June	1.31	0.82	0.76	0.86	3.17	–7.66	–3.14	–0.89
July	0.81	1.20	1.06	1.49	–2.46	2.27	–0.69	7.03
August	0.00	0.37	1.13	1.10	–14.36	–11.60	0.42	0.52
September	0.00	0.27	0.90	1.13	–14.80	–15.16	–2.69	–0.96
October	0.67	0.79	0.70	1.26	–5.33	–4.11	–5.98	3.33
November	3.79	0.81	0.86	1.45	22.97	–4.76	–4.21	5.93
December	3.67	0.17	1.16	1.83	35.01	–19.53	1.73	12.74

REMA: Red Estatal de Monitoreo Atmosférico (State Ambient Air Monitoring Network); CAMS: Copernicus Atmospheric Monitoring Service.

Table IV. Scaling factors by adjustment ratio and average monthly difference of PM_{10}.

Month	Using ratio (REMA/CAMS) monthly average of PM_{10}					Using difference (REMA – CAMS) monthly average of PM_{10}				
	Agua Santa	BINE	Ninfas	UTP	Velódromo	Agua Santa	BINE	Ninfas	UTP	Velódromo
January	na	2.02	3.03	4.12	1.95	n.a.	15.56	62.15	65.00	19.53
February	3.19	6.46	5.32	6.58	2.73	31.12	60.56	78.09	74.65	20.98
March	4.96	2.71	3.65	4.20	1.68	72.43	42.40	71.73	71.88	14.14
April	4.55	2.42	3.07	3.48	0.08	78.76	39.93	76.45	69.27	–37.01
May	3.23	1.71	1.87	2.57	0.00	45.04	15.87	24.36	46.26	–35.49
June	2.23	1.41	1.87	1.08	0.00	23.49	0.18	17.60	5.01	–28.62
July	1.19	2.15	2.78	3.04	0.00	4.33	20.32	40.77	45.42	–28.81
August	n.a.	1.68	2.53	2.53	0.00	n.a.	10.77	28.95	27.77	–25.94
September	n.a.	1.54	1.69	2.28	0.00	n.a.	8.08	12.48	25.52	–27.72
October	0.92	1.81	1.74	2.15	0.00	–2.18	16.89	15.57	22.68	–27.37
November	6.01	3.15	1.60	2.83	0.00	62.57	32.94	18.32	38.11	–19.19
December	6.11	3.09	2.36	3.58	0.00	101.35	58.65	48.84	61.41	–31.44

REMA: Red Estatal de Monitoreo Atmosférico (State Ambient Air Monitoring Network); CAMS: Copernicus Atmospheric Monitoring Service; n.a.: not applicable.

For January, both methods show significant differences in the Ninfas and UTP stations, where the ratio method detects more exceedances than the difference method. This trend persists across most months, with the ratio method generally showing more frequent exceedances. February and March show relatively high exceedances across all stations, with the ratio method consistently identifying more exceedances in Agua Santa and Velódromo compared to the difference method. Both methods show

Table V. Adjustment for difference and ratio of AHI for $PM_{2.5}$.

Month	$PM_{2.5}$ CAMS Adjustment for difference				$PM_{2.5}$ CAMS Adjustment by ratio			
	Number of times AHI > 45 µg m^{-3}				Number of times AHI > 45 µg m^{-3}			
	Agua Santa	BINE	Ninfas	UTP	Agua Santa	BINE	Ninfas	UTP
January	0	0	1	0	0	3	5	2
February	0	1	1	0	0	0	11	1
March	5	4	1	2	0	1	9	3
April	15	3	4	4	18	14	8	11
May	2	1	2	3	11	1	2	10
June	0	1	0	0	0	1	0	0
July	0	0	0	0	0	1	0	1
August	0	1	0	0	0	0	0	0
September	0	0	0	0	0	0	0	0
October	0	0	0	0	0	0	0	0
November	0	1	0	0	8	0	0	0
December	24	0	0	1	18	0	0	4

Table VI. Adjustment for difference and ratio of AHI for PM_{10}.

Month	PM_{10} CAMS Adjustment for difference					PM_{10} CAMS Adjustment by ratio				
	Number of times AHI > 75 µg m^{-3}					Number of times AHI > 75 µg m^{-3}				
	Agua Santa	BINE	Ninfas	UTP	Velódromo	Agua Santa	BINE	Ninfas	UTP	Velódromo
January	0	1	31	30	4	0	16	24	26	15
February	0	23	28	28	0	14	21	26	25	4
March	29	16	29	29	1	22	20	24	25	7
April	30	19	30	30	0	26	21	27	25	1
May	11	1	5	20	0	16	11	10	19	0
June	0	0	0	0	0	2	1	1	0	0
July	0	1	7	5	0	0	10	14	12	0
August	0	0	0	0	0	0	3	4	4	0
September	0	0	0	0	0	0	2	0	4	0
October	0	0	0	0	0	0	3	0	0	0
November	15	1	2	3	0	15	8	4	7	0
December	29	27	29	31	0	28	23	24	25	0

AHI: air and health indices; CAMS: Copernicus Atmospheric Monitoring Service.

consistently high exceedances across most stations in April, particularly in Ninfas and UTP. However, the Velódromo station shows no exceedances using the difference method, whereas the ratio method still detects some. May through August display fewer exceedances overall, with the ratio method continuing to detect a few cases, while the difference method shows almost none. June through September sees almost no exceedances for either method, with the few that occur primarily identified by the ratio method. In November and December, both methods show significant exceedances at stations like Agua Santa, Ninfas, and UTP, but again, the ratio method generally identifies more exceedances.

The ratio-based adjustment tends to detect more instances where the PM_{10} concentration exceeds the

75 μg m^{-3} threshold compared to the difference-based method, suggesting that it may be more sensitive in identifying higher pollution levels across the various monitoring stations.

3.2 Comparison of the REMA persistence forecast with the CAMS forecast

The analysis carried out in Tables V and VI allows us to determine that the ratio adjustment is appropriate for predicting events of poor air quality of $PM_{2.5}$ and PM_{10}.

A comparison between the persistence forecast of REMA concentrations and the ratio-adjusted CAMS forecast allows evaluation of the performance of CAMS relative to the REMA persistence forecast. This evaluation is presented in Tables VII, VIII, IX, X, XI, and XII.

Tables VII and VIII show that the highest $PM_{2.5}$ concentration levels are observed during the hot-dry season (March-May) and the cold-dry season (November-January). The CAMS adjustment by ratio results in a higher number of events where concentrations exceed 45 μg m^{-3}. In the hot-dry season, the Agua Santa (April and May), BINE (April), Ninfas (February), and UTP (April and May) stations are the most affected. The Agua Santa station is the most affected in the cold-dry season (November and December). However, in the hot-dry season, the persistence forecast exceeds the CAMS only at the BINE station in February and March.

Table IX shows that the lowest levels of $PM_{2.5}$ concentrations occur in the rainy season. The REMA persistence forecast results in more events than the CAMS ratio adjustment.

Tables X and XI show that the highest levels of PM_{10} concentrations occur in the hot-dry and cold-dry seasons. The CAMS ratio adjustment includes a more significant number of times that the AHI is greater than 75 μg m^{-3} at the Agua Santa and BINE stations. The persistence forecast is higher at the

Table VII. REMA persistence forecast and ratio-adjusted CAMS forecast for the hot-dry season of $PM_{2.5}$.

Month	REMA $PM_{2.5}$ persistence forecast				CAMS $PM_{2.5}$ forecast ratio adjustment			
	Number of times AHI > 45 μg m^{-3}				Number of times AHI > 45 μg m^{-3}			
	Agua Santa	BINE	Ninfas	UTP	Agua Santa	BINE	Ninfas	UTP
February	1	3	0	1	0	0	11	1
March	10	4	3	2	0	1	9	3
April	15	4	1	2	18	14	8	11
May	5	0	0	0	11	1	2	10

REMA: Red Estatal de Monitoreo Atmosférico (State Ambient Air Monitoring Network); CAMS: Copernicus Atmospheric Monitoring Service.

Table VIII. REMA persistence forecast and ratio-adjusted CAMS forecast for the cold-dry season of $PM_{2.5}$

Month	REMA $PM_{2.5}$ persistence forecast				CAMS $PM_{2.5}$ forecast ratio adjustment			
	Number of times AHI > 45 μg m^{-3}				Number of times AHI > 45 μg m^{-3}			
	Agua Santa	BINE	Ninfas	UTP	Agua Santa	BINE	Ninfas	UTP
January	0	0	2	2	0	3	5	2
November	4	1	0	0	8	0	0	0
December	17	0	2	1	18	0	0	4

REMA: Red Estatal de Monitoreo Atmosférico (State Ambient Air Monitoring Network); CAMS: Copernicus Atmospheric Monitoring Service; AHI: air and health indices.

Table IX. REMA persistence forecast and ratio-adjusted CAMS forecast for the rainy season of $PM_{2.5}$

Month	REMA $PM_{2.5}$ persistence forecast				CAMS $PM_{2.5}$ forecast ratio adjustment			
	Number of times AHI > 45 µg m^{-3}				Number of times AHI > 45 µg m^{-3}			
	Agua Santa	BINE	Ninfas	UTP	Agua Santa	BINE	Ninfas	UTP
June	0	0	0	1	0	1	0	0
July	0	2	0	1	0	1	0	1
August	0	0	0	0	0	0	0	0
September	0	0	0	1	0	0	0	0
October	0	1	0	0	0	0	0	0

REMA: Red Estatal de Monitoreo Atmosférico (State Ambient Air Monitoring Network); CAMS: Copernicus Atmospheric Monitoring Service; AHI: air and health indices.

Table X. REMA persistence forecast and ratio-adjusted CAMS forecast for the hot-dry season of PM_{10}.

Month	REMA PM_{10} persistence forecast					CAMS PM_{10} forecast ratio adjustment				
	Number of times AHI > 75 µg m^{-3}					Number of times AHI > 75 µg m^{-3}				
	Agua Santa	BINE	Ninfas	UTP	Velódromo	Agua Santa	BINE	Ninfas	UTP	Velódromo
February	11	18	24	23	9	14	21	26	25	4
March	25	19	25	26	12	22	20	24	25	7
April	27	18	28	23	1	26	21	27	25	1
May	10	3	6	16	0	16	11	10	19	0

REMA: Red Estatal de Monitoreo Atmosférico (State Ambient Air Monitoring Network); CAMS: Copernicus Atmospheric Monitoring Service; AHI: air and health indices.

Table XI. REMA persistence forecast and ratio-adjusted CAMS forecast for the cold-dry season of PM_{10}.

Month	REMA PM_{10} persistence forecast					CAMS PM_{10} forecast ratio adjustment				
	Number of times AHI > 75 µg m^{-3}					Number of times AHI > 75 µg m^{-3}				
	Agua Santa	BINE	Ninfas	UTP	Velódromo	Agua Santa	BINE	Ninfas	UTP	Velódromo
November	9	5	5	9	0	15	8	4	7	0
December	23	18	21	23	0	28	23	24	25	0
January	0	6	19	22	5	0	16	24	26	15

REMA: Red Estatal de Monitoreo Atmosférico (State Ambient Air Monitoring Network); CAMS: Copernicus Atmospheric Monitoring Service; AHI: air and health indices.

UTP and Velódromo stations and has a similar value at the Ninfas station of the atmospheric monitoring network.

Table XII compares the number of days with PM_{10} levels above 75 µg m^{-3} between the REMA PM_{10} persistence forecast and the CAMS PM_{10} forecast (ratio adjustment) for five stations (Agua Santa, BINE, Ninfas, UTP, and Velódromo) across the rainy season. Both forecasts recorded few exceedances in June, with similar numbers between the stations. July saw

Table XII. REMA persistence forecast and ratio-adjusted CAMS forecast for the rainy season of PM_{10}

Month	REMA PM_{10} persistence forecast					CAMS PM_{10} forecast ratio adjustment				
	Number of times AHI > 75 µg m^{-3}					Number of times AHI > 75 µg m^{-3}				
	Agua Santa	BINE	Ninfas	UTP	Velódromo	Agua Santa	BINE	Ninfas	UTP	Velódromo
June	1	1	2	4	0	2	1	1	0	0
July	2	7	9	14	0	0	10	14	12	0
August	0	0	1	4	0	0	3	4	4	0
September	0	2	1	5	0	0	2	0	4	0
October	2	2	1	1	0	0	3	0		0

REMA: Red Estatal de Monitoreo Atmosférico (State Ambient Air Monitoring Network); CAMS: Copernicus Atmospheric Monitoring Service; AHI: air and health indices.

higher exceedances in the persistence forecast, particularly at BINE, Ninfas, and UTP stations, whereas CAMS also had several exceedances but generally fewer. In August and September, exceedances were minimal in both forecasts, except for a few at UTP and Ninfas. October had minimal exceedances in both forecasts, with no recorded exceedances at Velódromo.

3.3 Comparison of dichotomous statistics of Copernicus CAMS and REMA Persistence

Dichotomous statistics describe the characteristics of forecast performance. The obtaining process includes data from the CAMS AHI of PM_{10} and $PM_{2.5}$ adjusted by ratio and the concentrations of PM_{10} and $PM_{2.5}$ from REMA in the MZVP.

The comprehensive results of the dichotomous statistics are available in Tables SI to SXVIII in the supplementary material. They constitute the basis for evaluating dichotomous statistics. The objective is to establish the CAMS's fulfillment with respect to the REMA persistence forecast.

Table XIII represents the percentage proportion of values that record the monthly dichotomous statistics at the $PM_{2.5}$ monitoring stations. The percentage proportion indicates the number of hits close to or equal to the optimal value of the statistic in Table II. The comparison considers when CAMS is better

Table XIII. Percentage comparison of dichotomous CAMS and REMA persistence statistics adjusted by ratio for $PM_{2.5}$.

	Performance of CAMS ratio adjustment vs. REMA persistence forecast for $PM_{2.5}$										
	ACCURACY (%)	BIAS (%)	POD (%)	FAR (%)	POFD (%)	SR (%)	TS (%)	ETS (%)	HK (%)	HSS (%)	ORSS (%)
CAMS better than persistence	27.08	4.17	4.17	4.17	18.75	6.25	6.25	18.75	16.67	20.83	4.17
CAMS equal to persistence	37.50	2.08	27.08	16.67	41.67	16.67	25.00	6.25	6.25	2.08	14.58
Persistence better than CAMS	35.42	35.42	10.42	12.50	35.42	10.42	12.50	18.75	18.75	20.83	12.50

REMA: Red Estatal de Monitoreo Atmosférico (State Ambient Air Monitoring Network); CAMS: Copernicus Atmospheric Monitoring Service; ACCURACY: accuracy; BIAS: bias score; POD: probability of detection; FAR: false alarm rate; POFD: probability of false detection; SR: success ratio; TS: threat score; ETS: equitable threat score**;** HSS: Heidke skill score; ORSS: odds ratio skill score.

than persistence, CAMS is equal to persistence, and persistence is better than CAMS. The results indicate a more significant number of statistics with a higher percentage when CAMS equals persistence: accuracy (ACCURACY), probability of detection (POD), false alarm rate (FAR), probability of false detection (POFD), success ratio (SR), threat score (TS), and odds ratio skill score (ORSS). The ETS and HSS statistics show equal percentages for cases where the CAMS is better than persistence and persistence is better than CAMS. For the BIAS and HK statistics, persistence outperforms CAMS.

Table XIV presents the percentage proportion of values that the dichotomous statistics record monthly at the PM_{10} monitoring stations. The comparison considers when CAMS is better than persistence, CAMS is the same as persistence, and persistence is better than CAMS. The results indicate a higher percentage for all statistics when persistence is better than CAMS.

Next, a series of graphs depicts the average values of dichotomous statistics for each climatic season across the stations in the atmospheric monitoring network. The purpose is to determine which stations best represent the air quality of $PM_{2.5}$ and PM_{10} at a local and regional level. Stations with a better performance in the REMA persistence forecast are suited for describing local air quality, while those with better performance in the CAMS forecast are more suitable for characterizing regional air quality.

Figure 3 shows the dichotomous average value statistics for the hot-dry season of $PM_{2.5}$. The REMA persistence forecast performs better than CAMS at the Agua Santa, BINE, and Ninfas stations. At the UTP station, CAMS performs slightly better than the REMA persistence forecast. The Agua Santa, BINE, and Ninfas stations represent air quality at a local level, while the UTP station reflects air quality at the regional level.

Figure 4 shows the dichotomous average value statistics for the cold-dry season of $PM_{2.5}$. The Agua Santa station of CAMS is better than that of REMA, the Ninfas station of REMA is better than CAMS, and the BINE and UTP stations of REMA are slightly better than CAMS. The Agua Santa station describes air quality at the regional level, while the BINE and UTP stations reflect local air quality.

Figure 5 shows the dichotomous average value statistics of $PM_{2.5}$ for the rainy season. Due to the absence of data, CAMS and REMA generally present similarities, with a slight trend of improvement in the persistence forecast at the BINE and UTP stations. The BINE and UTP stations reflect local air quality.

Figure 6 shows the dichotomous average value statistics for the hot-dry season of PM_{10}. The REMA persistence forecast performs better than CAMS at

Table XIV. Percentage comparison of dichotomous CAMS and REMA persistence statistics adjusted by ratio for PM_{10}.

	Performance of CAMS ratio adjustment vs. REMA persistence forecast for PM_{10}										
	ACCURACY (%)	BIAS (%)	POD (%)	FAR (%)	POFD (%)	SR (%)	TS (%)	ETS (%)	HK (%)	HSS (%)	ORSS (%)
CAMS better than persistence	25.00	3.33	23.33	16.67	20.00	15.00	18.33	26.67	26.67	26.67	18.33
CAMS equal to persistence	21.67	3.33	15.00	11.67	31.67	15.00	13.33	1.67	1.67	1.67	10.00
Persistence better than CAMS	53.33	73.33	40.00	40.00	48.33	38.33	48.33	51.67	51.67	51.67	40.00

REMA: Red Estatal de Monitoreo Atmosférico (State Ambient Air Monitoring Network); CAMS: Copernicus Atmospheric Monitoring Service; ACCURACY: accuracy; BIAS: bias score; POD: probability of detection; FAR: false alarm rate; POFD: probability of false detection; SR: success ratio; TS: threat score; ETS: equitable threat score**;** HSS: Heidke skill score; ORSS: odds ratio skill score.

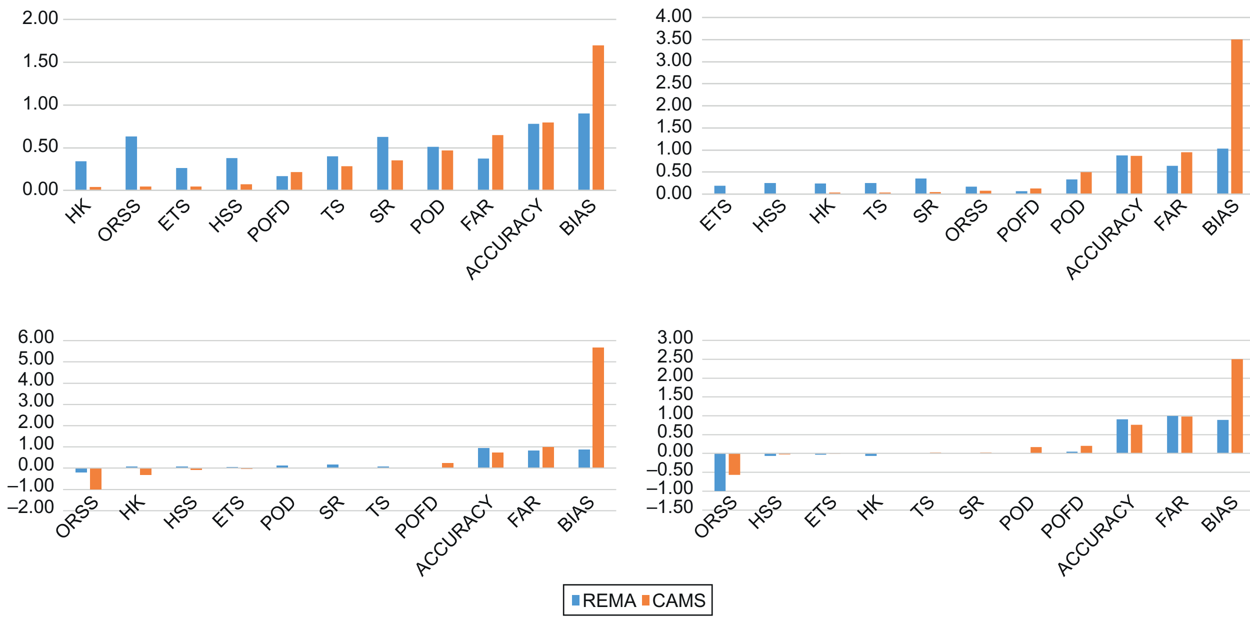

Fig. 3. Dichotomous statistics average value of $PM_{2.5}$ for the hot-dry season.

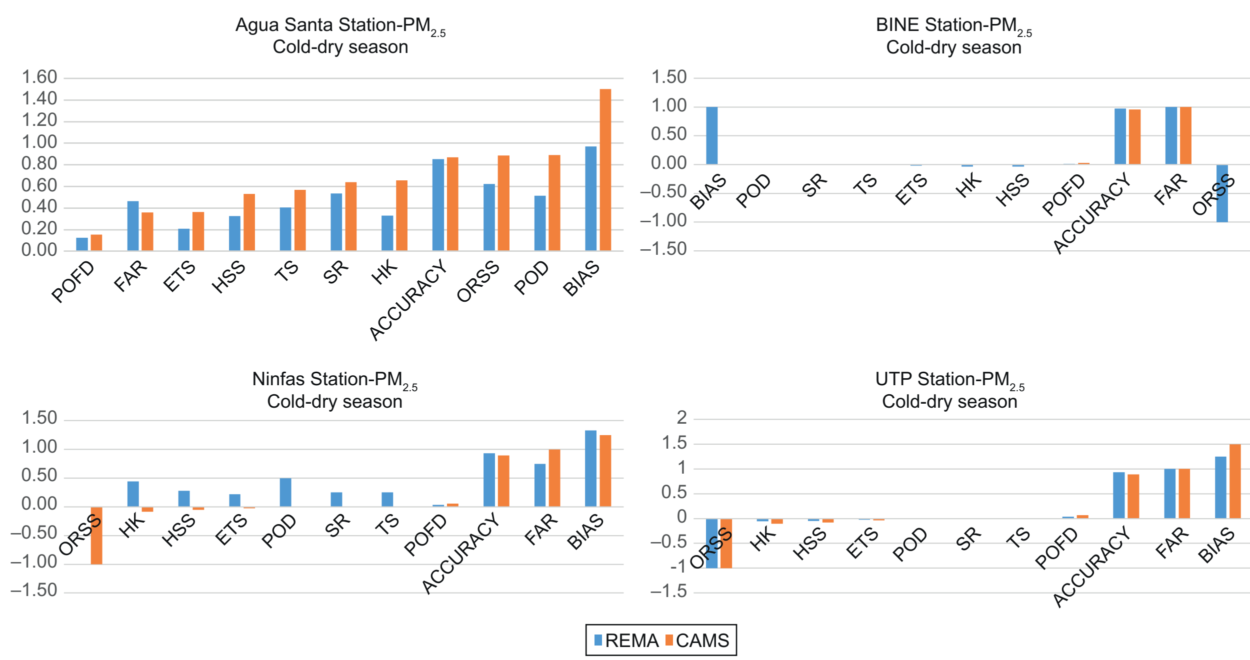

Fig. 4. Dichotomous statistics average value of $PM_{2.5}$ for the cold-dry season.

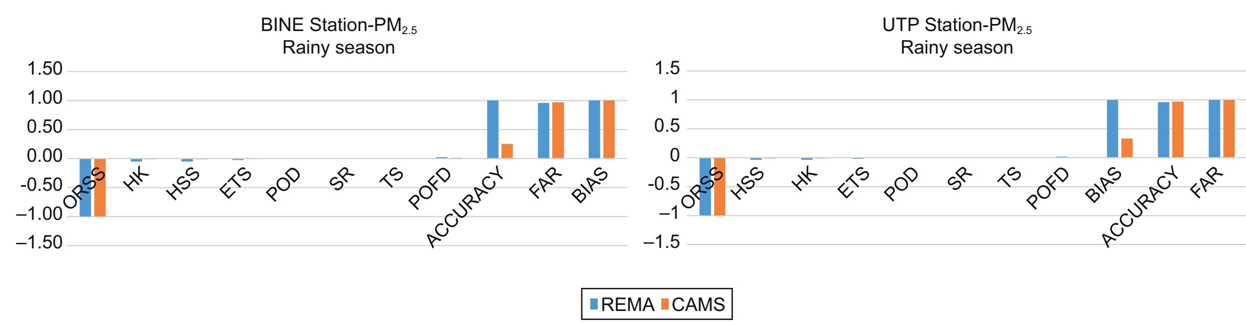

Fig. 5. Dichotomous statistics average value of $PM_{2.5}$ for the rainy season.

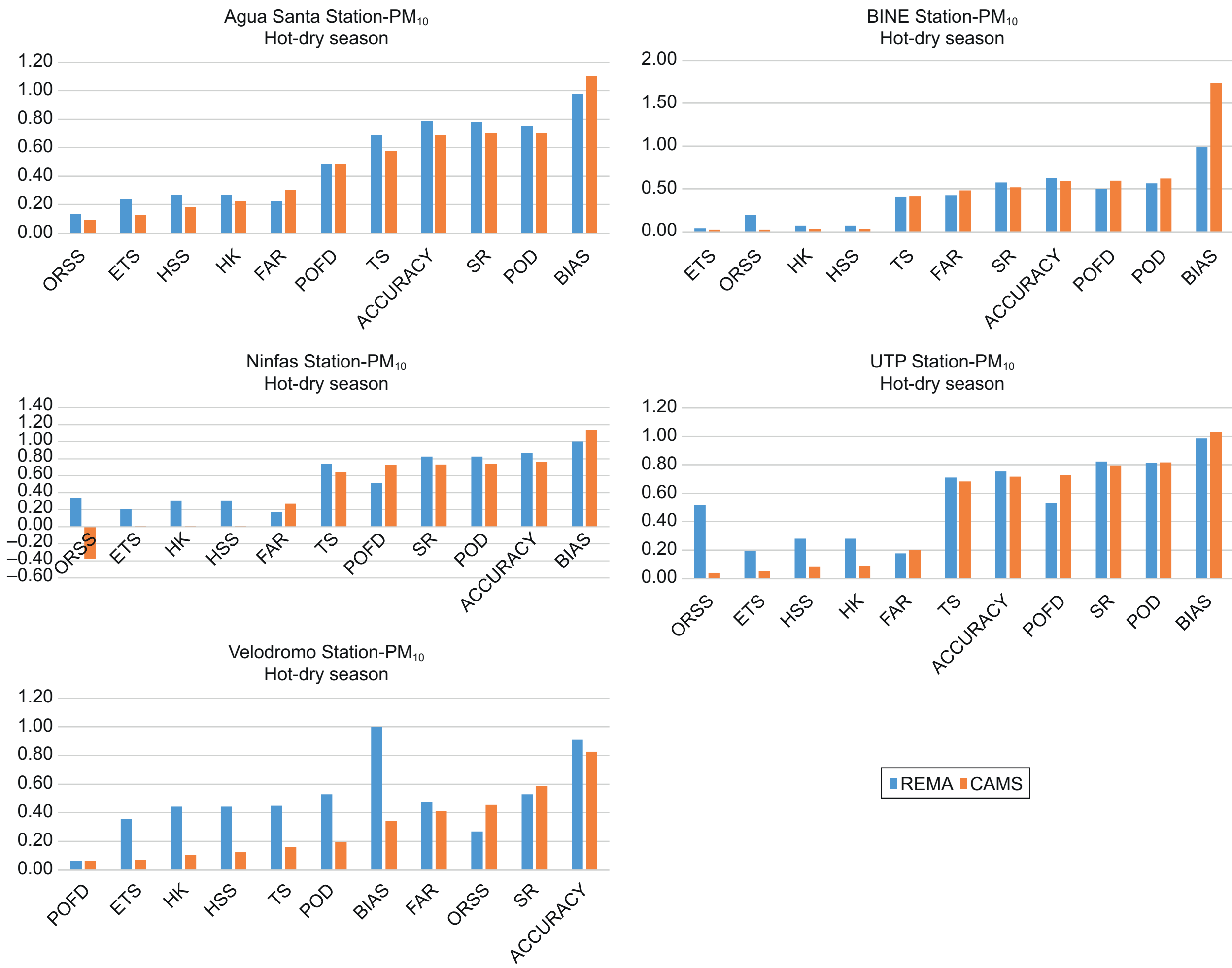

Fig. 6. Dichotomous statistics average value of PM_{10} for the hot-dry season.

the Agua Santa, BINE, Ninfas, UTP, and Velódromo stations, which represent air quality at the local level.

Figure 7 shows the dichotomous statistical average values for the cold-dry season of PM_{10}. At the Agua Santa, Ninfas, and UTP stations, the REMA persistence forecast performs better than CAMS. However, at the BINE and Velódromo stations, CAMS performs better than the REMA persistence forecast. The Agua Santa, Ninfas, and UTP stations describe the local air quality, and the BINE and Velódromo stations represent the regional air quality.

Figure 8 presents the dichotomous average value statistics for the rainy season of PM_{10}. At the Agua Santa, BINE, Ninfas, and UTP stations, the REMA persistence forecast performs better than CAMS. The Agua Santa, BINE, Ninfas, UTP, and Velódromo stations represent local air quality.

4. Conclusions

Our study presents a substantial advance in forecasting air quality within the MZVP. We have successfully implemented a procedure that effectively addresses systematic errors in the retrieval of CAMS forecast data. The results allow accurate predictions of poor air quality events aligned with the NOM-172-SEMARNAT-2019 standards.

Our findings demonstrate that ratio adjustment, applied to both PM_{10} and $PM_{2.5}$, significantly improves the CAMS's forecast performance. This adjustment outperforms the REMA persistence forecast for some periods and seasons by accurately predicting unsatisfactory air quality events attributed to PM_{10} and $PM_{2.5}$.

Furthermore, monthly percentage comparisons of dichotomous statistics reveal nuanced information.

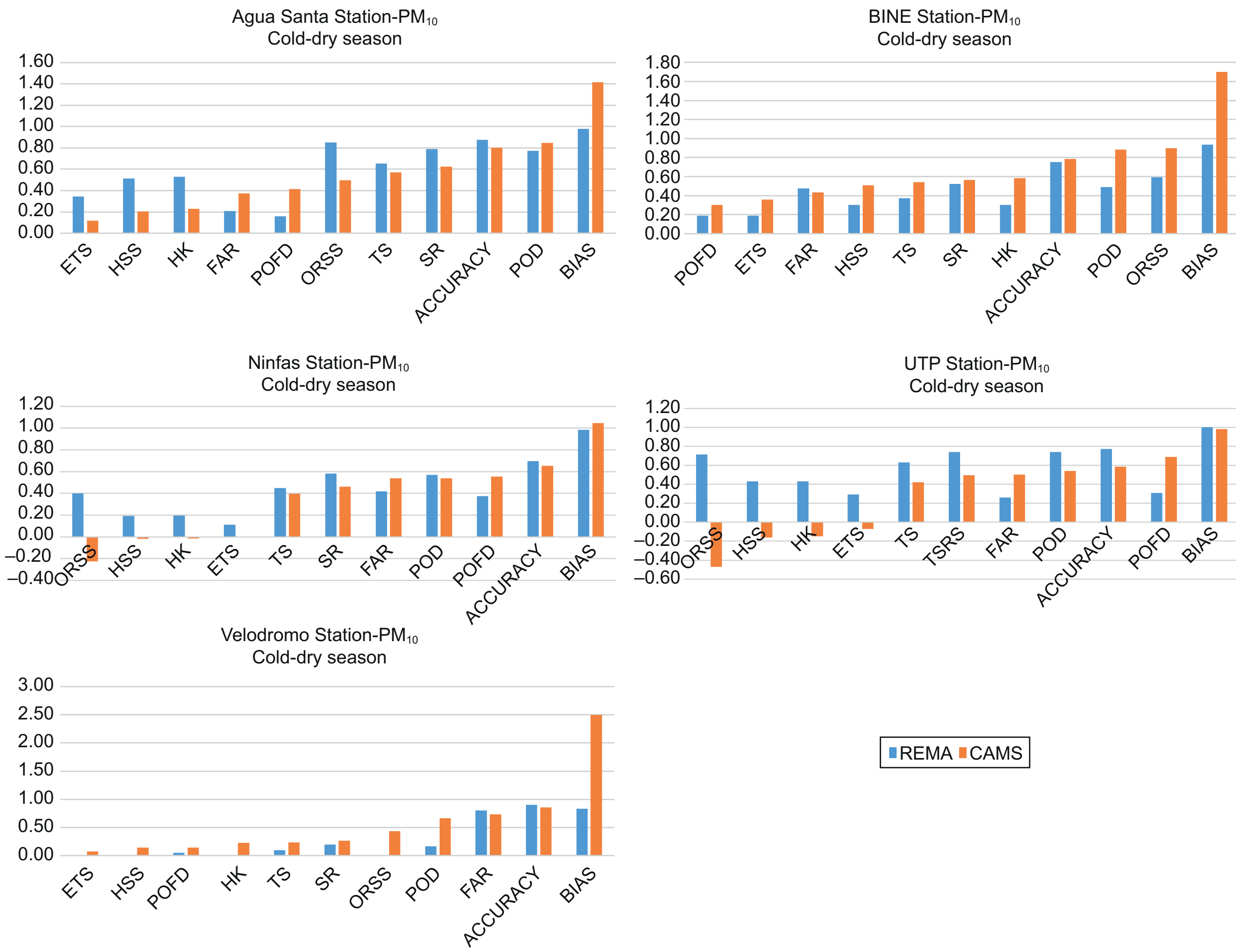

Fig. 7. Dichotomous statistics average value of PM_{10} for the cold-dry season.

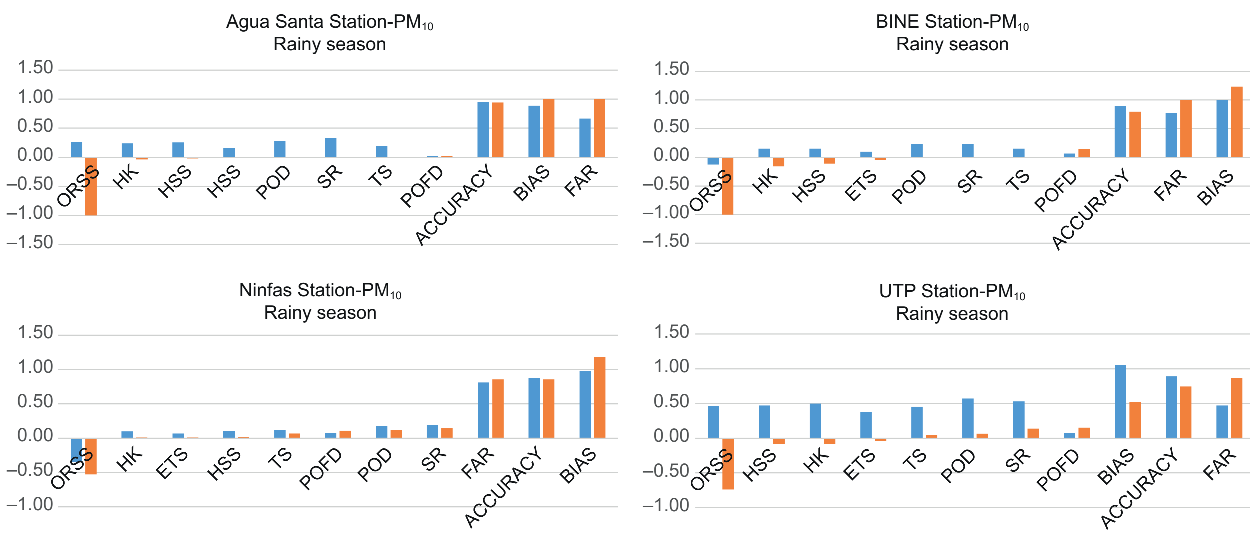

Fig. 8. Dichotomous statistics average value of PM_{10} for the rainy season.

At the same time, persistence outperforms CAMS in most cases for both $PM_{2.5}$ and PM_{10}. In a preliminary evaluation of the CAMS $PM_{2.5}$, it is possible to include specific statistics (ACCURACY, POD, FAR, POFD, SR, TS, ETS, HSS, and ORSS) in the forecast performance at the stations of the REMA. These statistics demonstrated acceptable percentages.

A more detailed analysis of the $PM_{2.5}$ forecasts from the UTP and Agua Santa stations as diagnostic indicators of poor-quality environmental $PM_{2.5}$ events indicates that they likely represent regional problems. These stations exhibit the highest average values in the dichotomous statistics for the hot-dry and cold-dry seasons, respectively. In contrast, the BINE and Ninfas stations are more representative of local problems, potentially influenced by local emissions, roads, and industrial factors. Regarding the PM_{10} forecasts, the BINE and Velódromo stations presented the highest average value of the dichotomous statistics for the cold-dry season.

The extended non-operational status of certain REMA stations resulted in insufficient data for the study. The scarcity of data for $PM_{2.5}$ (48.38%) and PM_{10} (37.12%) limited the exhaustiveness of our analysis.

The importance of our study lies in its pioneering approach. It is the first time such a complete comparison has been made on the American continent, specifically in Mexico. These findings provide critical information and suggest avenues for further improvement, including improving resolution, incorporating detailed emissions inventories, and accounting for local meteorological variables.

Our research lays the foundation for improving air quality forecasting in the region, offering valuable information for policy decisions and additional studies to enhance air quality in the MZVP.

Acknowledgments

Javier Omar Castillo-Miranda thanks the Consejo Nacional de Humanidades, Ciencias y Tecnologías (CONAHCyT) for the postdoctoral fellowship that supported this study. Additionally, both Javier Omar Castillo-Miranda and José Carlos Mendoza-Hernández acknowledge the Colegio de Ingeniería Ambiental of the Benemérita Universidad Autónoma de Puebla. Thanks are also extended to the Dirección de Gestión de la Calidad del Aire, Secretaría del Medio Ambiente Desarrollo Sustentable y Ordenamiento Territorial, Gobierno del Estado de Puebla, for providing valuable information for this project. The authors also acknowledge the reviewers for their time and comments. This work contains modified information from the Copernicus Atmosphere Monitoring Service (2021).

References

Benedetti A, Morcrette JJ, Boucher O, Dethof A, Engelen RJ, Fisher M, Flentje H, Huneeus N, Jones L, Kaiser JW, Kinne S, Mangold A, Razinger M, Simmons AJ, Suttie M. 2009. Aerosol analysis and forecast in the European Centre for Medium-Range Weather Forecasts Integrated Forecast System. 2: Data assimilation. Journal of Geophysical Research 114: D13205. https://doi.org/10.1029/2008JD011115

CAMS. 2023. CAMS global atmospheric composition forecasts. The Copernicus Atmosphere Monitoring Service. Available at: https://ads.atmosphere.copernicus.eu/datasets/cams-global-atmospheric-composition-forecasts?tab=overview (accessed 17 July 2023)

Cohen AJ, Brauer M, Burnett R, Anderson HR, Frostad J, Estep K, Balakrishnan K, Brunekreef B, Dandona L, Dandona R, Feigin V, Freedman G, Hubbell B, Jobling A, Kan H, Knibbs L, Liu Y, Martin R, Morawska L, Pope III CA, Shin H, Straif K, Shaddick G, Thomas M, Van Dingenen R, Van Donkelaar A, Vos T, Murray CJL, Forouzanfar MH†. 2017. Estimates and 25-year trends of the global burden of disease attributable to ambient air pollution: An analysis of data from the Global Burden of Diseases Study 2015. The Lancet 389: 1907-1918. https://doi.org/10.1016/S0140-6736(17)30505-6

Eskes H, Huijnen V, Arola A, Benedictow A, Blechschmidt A-M, Botek E, Boucher O, Bouarar I, Chabrillat S, Cuevas E, Engelen R, Flentje H, Gaudel A, Griesfeller J, Jones L, Kapsomenakis J, Katragkou E, Kinne S, Langerock B, Razinger M, Richter A, Schultz M, Schulz M, Sudarchikova N, Thouret V, Vrekoussis M, Wagner A, Zerefos C. 2015. Validation of reactive gases and aerosols in the MACC global analysis and forecast system. Geoscientific Model Development 8: 3523-3543. https://doi.org/10.5194/gmd-8-3523-2015

Flemming J, Peuch VH, Engelen R, Kaiser JW. 2013. A European global-to-regional air pollution forecasting system that combines modeling with satellite observations. EM Magazine of A&WMA 2013: 6-10. Available at: https://www.researchgate.net/publication/259535688_A_European_Global-to Regional_Air_Pollution_Forecasting_System_that_Combines_Modeling_with_Satellite_Observations (accessed 2023 February 28).

Gold S, White E, Roeder W, McAleenan M, Kabban CS, Ahner D. 2020. Probabilistic contingency tables: An improvement to verify probability forecasts. Weather and Forecasting 35: 609-621. https://doi.org/10.1175/WAF-D-19-0116.1

Granier C, Bessagnet B, Bond T, D'Angiola A, Denier van der Gon H, Frost GJ, Heil A, Kaiser JW, Kinne S, Klimont Z, Kloster S, Lamarque JF, Liousse C, Masui T, Meleux F, Mieville A, Ohara T, Raut JC, Riahi K, Schultz MG, Smith SJ, Thompson A, van Aardenne J, van der Werf GR, van Vuuren DP. 2011. Evolution of anthropogenic and biomass burning emissions of air pollutants at global and regional scales during the 1980-2010 period. Climate Change 109: 163. https://doi.org/10.1007/s10584-011-0154-1

Green J, Sánchez S. 2013. La calidad del aire en América Latina: una visión panorámica. Clean Air Institute, Washington DC, USA. Available at: https://naturalezasintoxicos.wordpress.com/wp-content/uploads/2013/10/cai-report-spanish.pdf (accessed 2023 February 14)

Hollingsworth A, Engelen RJ, Textor C, Benedetti A, Boucher O, Chevallier F, Dethof A, Elbern H, Eskes H, Flemming J, Granier C, Kaiser JW, Morcrette JJ, Rayner P, Peuch VH, Rouil L, Schultz MG, Simmons AJ. 2008. Toward a monitoring and forecasting system for atmospheric composition. The GEMS project. Bulletin of the American Meteorological Society 89: 1147-1164. https://doi.org/10.1175/2008BAMS2355.1

IHME. 2024. Air Pollution. Institute for Health Metrics and Evaluation. Available at: https://www.healthdata.org/research-analysis/health-risks-issues/air-pollution (accessed 18 October 2024).

INECC. 2019. Informe Nacional de Calidad del Aire 2018, México. Instituto Nacional de Ecología y Cambio Climático, Mexico. Available at: https://sinaica.inecc.gob.mx/archivo/informes/Informe2018.pdf (accessed 2023 February 28).

INECC. 2020. Informe Nacional de la Calidad del Aire 2019, México. Instituto Nacional de Ecología y Cambio Climático, Mexico. Available at: https://sinaica.inecc.gob.mx/archivo/informes/Informe2019.pdf (accessed 2023 March 15).

INEGI. 2017. Publicaciones: Anuario estadístico y geográfico de Puebla 2017. Instituto Nacional de Estadística y Geografía, Mexico. Available at: https://www.inegi.org.mx/app/biblioteca/ficha.html?upc=702825094973 (accessed 2023 March 23)

INEGI. 2018. Mapas: conjunto de datos vectoriales de uso del suelo y vegetación. Escala 1:250 000. Serie VII. Conjunto nacional. Instituto Nacional de Estadística y Geografía, Aguascalientes, Mexico. Available at: https://www.inegi.org.mx/app/biblioteca/ficha.html?upc=889463842781 (accessed 2023 March 30)

Kalita G, Yadav PP, Jat R, Govardhan G, Ambulkar R, Kumar R, Gunwani P, Debnath S, Sharma P, Kulkarni S, Kaginalkar A, Ghude SD. 2023. Forecasting of an unusual dust event over western India by the Air Quality Early Warning System. Atmospheric Environment 311: 120013. https://doi.org/10.1016/j.atmosenv.2023.120013

Kloog I, Ridgway B, Koutrakis P, Coull BA, Schwartz JD. 2013. Long- and short-term exposure to $PM_{2.5}$ and mortality using novel exposure models. Epidemiology 24: 555-561. https://doi.org/10.1097/EDE.0b013e318294beaa

Kukkonen J, Olsson T, Schultz DM, Baklanov A, Klein T, Miranda AI, Monteiro A, Hirtl M, Tarvainen V, Boy M, Peuch VH, Poupkou A, Kioutsioukis I, Finardi S, Sofiev M, Sokhi R, Lehtinen KEJ, Karatzas K, San José R, Astitha M, Kallos G, Schaap M, Reimer E, Jakobs H, Eben K. 2012. A review of operational, regional-scale, chemical weather forecasting models in Europe. Atmospheric Chemistry and Physics 12: 1-87. https://doi.org/10.5194/acp-12-1-2012

MacNee W, Donalson K. 2000. Exacerbations of COPD: Environmental mechanisms. Chest 117: 390S-397S. https://doi.org/10.1378/chest.117.5_suppl_2.390S

Morcrette JJ, Boucher O, Jones L, Salmond D, Bechtold P, Beljaars A, Benedetti A, Bonet A, Kaiser JW, Razinger M, Schulz M, Serrar S, Simmons AJ, Sofiev M, Suttie M, Tompkins AM, Untch A. 2009. Aerosol analysis and forecast in the European Centre for Medium-Range Weather Forecasts Integrated Forecast System: Forward modeling. Journal of Geophysical Research 115: D06206. https://doi.org/10.1029/2008JD011235

PAHO. 2024. Air quality. Pan American Health Organization. Available at: https://www.paho.org/en/topics/air-quality (accessed 20 October 2024).

Pappa A, Kioutsioukis I. 2021. Forecasting particulate pollution in an urban area: From Copernicus to sub-km scale. Atmosphere 12: 881. https://doi.org/10.3390/atmos12070881

PMD. 2011. Plan Municipal de Desarrollo (PMD) del Municipio de Puebla 2011-2014. H. Ayuntamiento de Puebla, Mexico. Available at: https://memorias.pueblacapital.gob.mx/vi-planes-municipales-de-desarrollo/174-planes-municipales-de-desarrollo/3687-2011-2014-planes-municipales-de-desarrollo (accessed 2024 November 8).

PMD. 2021. Plan Municipal de Desarrollo (PMD) del Municipio de Puebla 2021-2024. Ayuntamiento de Puebla, Mexico. Available at: https://ojp.puebla.gob.mx/normatividad-municipal/item/3778-plan-municipal-de-desarrollo-de-puebla-puebla-2021-2024 (accessed 2023 April 25).

Pope CAIII, Burnett RT, Thurston GD, Thun MJ, Calle EE, Krewski D, Godleski JJ. 2004. Cardiovascular mortality and long-term exposure to particulate air pollution: Epidemiological evidence of general pathophysiological pathways of disease. Circulation 109: 71-77. https://doi.org/10.1161/01.CIR.0000108927.80044.7F

REDIM. 2013. Diagnóstico de fuentes de información sobre calidad del aire y derecho a la salud de niñas, niños y adolescentes en México. Red por los Derechos de la Infancia en México. Available at: https://aularedim.net/wp-content/uploads/22DiagnosticoAireLimpio.pdf (accessed 2023 April 30).

REMA. 2023. Índice aire y salud: históricos. Red Estatal de Monitoreo Atmosférico, Puebla, Mexico. Available at https://calidaddelaire.puebla.gob.mx/views/principal_monitoreo.php (accessed 20 February 2023).

Samet JM, Dominici F, Curriero FC, Coursac I, Zeger SL. 2000. Fine particulate air pollution and mortality in 20 U.S. cities, 1987-1994. The New England Journal of Medicine 343: 1742-1749. https://doi.org/10.1056/NEJM200012143432401

SEDEMA. 2020. Calidad del aire en la Ciudad de México. Informe 2018. Secretaría del Medio Ambiente de la Ciudad de México. Available at: http://www.aire.cdmx.gob.mx/descargas/publicaciones/informe-anual-calidad-del-aire-2018.pdf (accessed 2023 May 5).

SEMARNAT. 2019. Norma Oficial Mexicana NOM-172-SEMARNAT-2019. Lineamientos para la obtención y comunicación del Índice de Calidad del Aire y Riesgos a la Salud. Secretaría de Medio Ambiente y Recursos Naturales, Diario Oficial de la Federación, Mexico, November 20.

Shaddick G, Thomas ML, Amini H, Broday D, Cohen A, Frostad J, Green A, Gumy S, Liu Y, Martin RV, Prüss-Üstün A, Simpson D, Van Donkelaar A, Brauer M. 2018. Data integration for the assessment of population exposure to ambient air pollution for global burden of disease assessment. Environmental Science & Technology 52: 9069-9078. https://doi.org/10.1021/acs.est.8b02864

SMADSOT. 2021. Informe anual de calidad del aire Zona Metropolitana del Valle de Puebla. Del 01 de enero al 31 de diciembre de 2021. Diagnóstico de contaminantes criterio. Partículas PM_{10} y $PM_{2.5}$, ozono, monóxido de carbono, bióxido de azufre y bióxido de nitrógeno en la Zona Metropolitana del Valle de Puebla (ZMVP). Secretaría de Medio Ambiente Desarrollo Sustentable y Ordenamiento Territorial, Puebla, Mexico. Available at: https://calidaddelaire.puebla.gob.mx/documents/Reporte_Anual_2021_Calidad_del_Aire.pdf (accessed 2023 May 15).

SMADSOT. 2023a. Incidencia de la contaminación atmosférica sobre la salud en el Estado de Puebla, 2023. Programa de Gestión de Calidad del Aire y de Acción ante el Cambio Climático, 2021-2030. Secretaría de Medio Ambiente Desarrollo Sustentable y Ordenamiento Territorial, Puebla, Mexico. Available at: https://calidaddelaire.puebla.gob.mx/documents/ProAire-PEACC_2021-2030/extensos/5-1-Incidencia-Salud.pdf (accessed 2024 October 21).

SMADSOT. 2023b. Base de datos de partículas PM_{10} y $PM_{2.5}$ de los años 2020 y 2021 de la Red Estatal de Monitoreo Atmosférico. Secretaría de Medio Ambiente, Desarrollo Sustentable y Ordenamiento Territorial del Gobierno del Estado de Puebla. Database USB drive.

USEPA. 2020. Annual report 2019: Our nation's air. United States Environmental Protection Agency. Available at: https://gispub.epa.gov/air/trendsreport/2020/documentation/AirTrends_Flyer.pdf (accessed 2023 May 10).

Wagner A, Blechschmidt A-M, Bouarar I, Brunke E-G, Clerbaux C, Cupeiro M, Cristofanelli P, Eskes H, Flemming J, Flentje H, George M, Gilge S, Hilboll A, Inness A, Kapsomenakis, J, Richter A, Ries L, Spangl W, Stein O, Weller R, Zerefos C. 2015. Evaluation of the MACC operational forecast system – Potential and challenges of global near-real-time modelling with respect to reactive gases in the troposphere. Atmospheric Chemistry and Physics 15: 14005-14030. https://doi.org/10.5194/acp-15-14005-2015

WHO. 2006. Air quality guidelines. Global update 2005. Particulate matter, ozone, nitrogen dioxide and sulfur dioxide. World Health Organization. Available at: https://iris.who.int/bitstream/handle/10665/107823/9789289021920-eng.pdf?sequence=1 (accessed 2023 June 1).

WHO. 2024. Ambient (outdoor) air pollution. World Health Organization. Available at: https://www.who.int/newsroom/fact-sheets/detail/ambient-(outdoor)-air-quality-and-health (accessed 23 October 2024).

WWRP-WGNE. 2017. Forecast verification methods across time and space scales. Methods for dichotomous (yes/no) forecasts. Joint Working Group on Forecast Verification Research. World Weather Research Programme-World Climate Research Programme. Available at: https://www.cawcr.gov.au/projects/verification/#Methods_for_dichotomous_forecasts (accessed 11 April 2023).

Zhang Y, Li Z, Chang W, Zhang Y, de Leeuw G, Schauer JJ. 2020. Satellite Observations of $PM_{2.5}$ Changes and Driving Factors Based Forecasting Over China 2000-2025. Remote Sensing 12: 2518. https://doi.org/10.3390/rs12162518

Supplementary material

S1. Description of dichotomous statistics

Accuracy (fraction correct): indicates the correct portion of the forecasts.

$$\text{Accuracy} = \frac{hits + correct\ negatives}{total} \quad (1)$$

Bias score (frequency bias): compares the frequency of the predicted events and the frequency of the observed events. Determines whether there is a tendency to under-forecast (BIAS < 1) or over-forecast (BIAS > 1) events.

$$\text{BIAS} = \frac{hits + false\ alarms}{hits + misses} \quad (2)$$

Probability of detection (hit rate): indicates the fraction of observed "yes" events that were correctly predicted.

$$\text{POD} = \frac{hits}{hits + misses} \quad (3)$$

False alarm rate: indicates the fraction of forecast events that will occur but did not occur.

$$\text{FAR} = \frac{false\ alarms}{hits + false\ alarms} \quad (4)$$

Probability of false detection (false alarm ratio): considers the part of events not observed that were incorrectly predicted as "yes".

$$\text{POFD} = \frac{false\ alarms}{correct\ negatives + false\ alarms} \quad (5)$$

Success ratio: considers the fraction of events predicted "yes" that were correctly observed.

$$\text{SR} = \frac{hits}{hits + false\ alarms} \quad (6)$$

Threat score (critical success rate): determines the part of observed and/or predicted events that were suitably predicted.

$$\text{TS} = \frac{hits}{hits + misses + false\ alarms} \quad (7)$$

Equitable threat score (Gilbert skill score): quantifies the portion of observed and/or predicted episodes that were suitably predicted, coupled by hits related to aleatory probability.

$$\text{ETS} = \frac{hits - hits_{random}}{hits + misses + false\ alarms - hits_{random}} \quad (8)$$

Where

$$hits_{random} = \frac{(hits + misses)(hits + false\ alarms)}{total} \quad (9)$$

Hanssen and Kuipers discriminant (true ability statistic, Peirce skill score): indicates the success of the forecast separating "yes" events from "no" events.

$$\text{HK} = -\frac{hits}{hits + misses}\ \frac{false\ alarms}{false\ alarms + correct\ negatives} \quad (10)$$

Heidke skill score (Cohen's K): establishes the share of correct predictions afterward, removing those forecasts that would be correct due to chance alone.

$$\frac{(hits + correct\ negatives) - (expected\ correct)_{random}}{N - (expected\ correct)_{random}} \quad (11)$$

where:

$$(expected\ correct)_{random} = 1/N\ [(hits + misses)(hits + false\ alarms) + (correct\ negatives + misses)(correc\ negatives + false\ alarms)] \quad (12)$$

Odds ratio skill score (Yule's Q): indicates how far the forecast was ahead of chance:

$$\text{ORSS} = \frac{hits * correct\ negatives - misses * false\ alarms}{hits * correct\ negatives + misses * false\ alarms} \quad (13)$$

S2. Comparison of dichotomous statistics of CAMS and REMA persistence

Tables SI, SII, SIII, SIV, XV, SVI, SVII, and SVIII compare the dichotomous statistics of the REMA persistence forecast with CAMS adjusted by ratio. It corresponds to $PM_{2.5}$ for the stations of the Atmospheric Monitoring Network in 2021.

Table SI. Comparison of dichotomous statistics of persistence air and REMA and CAMS health indices adjusted by ratio for $PM_{2.5}$ at the Agua Santa station.

	Dichotomous statistics, Agua Santa station $PM_{2.5}$											
	ACCURACY		BIAS		POD		FAR		POFD		SR	
Month	REMA	CAMS	REMA	CAMS	REMA	CAMS	REMA	CAMS	REMA	CAMS	REMA	CAMS
January	1.00	1.00	Null	Null	Null	Null	Null	Null	0.00	0.00	Null	Null
February	0.96	1.00	0.50	Null	0.50	Null	0.00	Null	0.00	0.00	1.00	Null
March	0.57	1.00	1.11	Null	0.33	Null	0.70	Null	0.33	0.00	0.30	Null
April	0.79	0.63	1.00	1.20	0.80	0.73	0.20	0.39	0.21	0.47	0.80	0.61
May	0.80	0.55	1.00	2.20	0.40	0.20	0.60	0.91	0.12	0.38	0.40	0.09
June	1.00	1.00	Null	Null	Null	Null	Null	Null	0.00	0.00	Null	Null
July	1.00	1.00	Null	Null	Null	Null	Null	Null	0.00	0.00	Null	Null
August	1.00	1.00	Null	Null	Null	Null	Null	Null	0.00	0.00	Null	Null
September	1.00	1.00	Null	Null	Null	Null	Null	Null	0.00	0.00	Null	Null
October	1.00	1.00	Null	Null	Null	Null	Null	Null	0.00	0.00	Null	Null
November	0.79	0.87	1.00	2.00	0.25	1.00	0.75	0.50	0.12	0.15	0.25	0.50
December	0.77	0.74	0.94	1.00	0.78	0.78	0.18	0.22	0.25	0.31	0.82	0.78

REMA: Red Estatal de Monitoreo Atmosférico (State Ambient Air Monitoring Network); CAMS: Copernicus Atmospheric Monitoring Service; Null = null value; ACCURACY: accuracy; BIAS: bias score; POD: probability of detection; FAR: false alarm rate; POFD: probability of false detection; SR: success ratio.

Table SII. Comparison of dichotomous statistics of persistence air and REMA and CAMS health indices adjusted by ratio for $PM_{2.5}$ at the Agua Santa station.

	Dichotomous statistics, Agua Santa station $PM_{2.5}$									
	TS		ETS		HK		HSS		ORSS	
Month	REMA	CAMS	REMA	CAMS	REMA	CAMS	REMA	CAMS	REMA	CAMS
January	Null	Null	Null	Null	Null	Null	Null	Null	Null	Null
February	0.50	Null	0.48	Null	0.50	Null	0.65	Null	1.00	Null
March	0.19	Null	0.00	Null	0.00	Null	0.00	Null	0.00	Null
April	0.67	0.50	0.41	0.15	0.59	0.27	0.59	0.27	0.87	0.52
May	0.25	0.07	0.16	–0.06	0.28	–0.18	0.28	–0.12	0.66	–0.43
June	Null	Null	Null	Null	Null	Null	Null	Null	Null	Null
July	Null	Null	Null	Null	Null	Null	Null	Null	Null	Null
August	Null	Null	Null	Null	Null	Null	Null	Null	Null	Null
September	Null	Null	Null	Null	Null	Null	Null	Null	Null	Null
October	Null	Null	Null	Null	Null	Null	Null	Null	Null	Null
November	0.14	0.50	0.07	0.42	0.13	0.85	0.13	0.59	0.42	1.00
December	0.67	0.64	0.35	0.31	0.53	0.47	0.52	0.47	0.83	0.77

REMA: Red Estatal de Monitoreo Atmosférico (State Ambient Air Monitoring Network); CAMS: Copernicus Atmospheric Monitoring Service; Null = null value; TS: threat score; ETS: equitable threat score**;** HSS: Heidke skill score; ORSS: odds ratio skill score.

Table SIII. Comparison of dichotomous statistics of REMA and CAMS persistence air and health indices adjusted by ratio for $PM_{2.5}$ at the BINE station.

	Dichotomous statistics, BINE station $PM_{2.5}$											
	ACCURACY		BIAS		POD		FAR		POFD		SR	
Month	REMA	CAMS	REMA	CAMS	REMA	CAMS	REMA	CAMS	REMA	CAMS	REMA	CAMS
January	1.00	0.90	Null	Null	Null	Null	Null	1.00	0.00	0.10	Null	0.00
February	0.81	1.00	0.75	Null	0.25	Null	0.67	Null	0.09	0.00	0.33	Null
March	0.77	0.97	1.33	Null	0.00	Null	1.00	1.00	0.15	0.03	0.00	0.00
April	0.93	0.53	1.00	3.50	0.75	0.50	0.25	0.86	0.04	0.46	0.75	0.14
May	1.00	0.97	Null	Null	Null	Null	Null	1.00	0.00	0.03	Null	0.00
June	1.00	0.97	Null	Null	Null	Null	Null	1.00	0.00	0.03	Null	0.00
July	0.87	0.90	1.00	0.50	0.00	0.00	1.00	1.00	0.07	0.03	0.00	0.00
August	1.00	1.00	Null	Null	Null	Null	Null	Null	0.00	0.00	Null	Null
September	1.00	1.00	Null	Null	Null	Null	Null	Null	0.00	0.00	Null	Null
October	0.93	0.97	1.00	0.00	0.00	0.00	1.00	Null	0.03	0.00	0.00	Null
November	0.93	0.97	1.00	0.00	0.00	0.00	1.00	Null	0.04	0.00	0.00	Null
December	1.00	1.00	Null	Null	Null	Null	Null	Null	0.00	0.00	Null	Null

REMA: Red Estatal de Monitoreo Atmosférico (State Ambient Air Monitoring Network); CAMS: Copernicus Atmospheric Monitoring Service; Null = null value; ACCURACY: accuracy; BIAS: bias score; POD: probability of detection; FAR: false alarm rate; POFD: probability of false detection; SR: success ratio.

Table SIV. Comparison of dichotomous statistics of REMA and CAMS persistence air and health indices adjusted by ratio for $PM_{2.5}$ at the BINE station.

	Dichotomous statistics, BINE station $PM_{2.5}$									
	TS		ETS		HK		HSS		ORSS	
Month	REMA	CAMS	REMA	CAMS	REMA	CAMS	REMA	CAMS	REMA	CAMS
January	Null	0.00	Null	0.00	Null	Null	Null	0.00	Null	Null
February	0.17	Null	0.10	Null	0.16	Null	0.18	Null	0.56	Null
March	0.00	0.00	–0.06	0.00	–0.15	Null	–0.13	0.00	–1.00	Null
April	0.60	0.13	0.55	0.01	0.71	0.04	0.71	0.02	0.97	0.08
May	Null	0.00	Null	0.00	Null	Null	Null	0.00	Null	Null
June	Null	0.00	Null	0.00	Null	Null	Null	0.00	Null	Null
July	0.00	0.00	–0.03	–0.02	–0.07	–0.03	–0.07	–0.04	–1.00	–1.00
August	Null	Null	Null	Null	Null	Null	Null	Null	Null	Null
September	Null	Null	Null	Null	Null	Null	Null	Null	Null	Null
October	0.00	0.00	–0.02	0.00	–0.03	0.00	–0.03	0.00	–1.00	Null
November	0.00	0.00	–0.02	0.00	–0.04	0.00	–0.04	0.00	–1.00	Null
December	Null	Null	Null	Null	Null	Null	Null	Null	Null	Null

REMA: Red Estatal de Monitoreo Atmosférico (State Ambient Air Monitoring Network); CAMS: Copernicus Atmospheric Monitoring Service; Null = null value; TS: threat score; ETS: equitable threat score**;** HSS: Heidke skill score; ORSS: odds ratio skill score.

Table SV**.** Comparison of dichotomous statistics of REMA and CAMS persistence air and health indices adjusted by ratio for $PM_{2.5}$ at the Ninfas station.

	Dichotomous statistics, Ninfas station $PM_{2.5}$											
	ACCURACY		BIAS		POD		FAR		POFD		SR	
Month	REMA	CAMS	REMA	CAMS	REMA	CAMS	REMA	CAMS	REMA	CAMS	REMA	CAMS
January	0.97	0.77	2.00	2.50	1.00	0.00	0.50	1.00	0.03	0.17	0.50	0.00
February	1.00	0.61	Null	4.50	Null	0.00	Null	1.00	0.00	0.35	Null	0.00
March	0.83	0.65	0.75	4.50	0.25	0.00	0.67	1.00	0.08	0.31	0.33	0.00
April	0.93	0.70	1.00	8.00	0.00	0.00	1.00	1.00	0.04	0.28	0.00	0.00
May	1.00	0.94	Null	Null	Null	Null	Null	1.00	0.00	0.06	Null	0.00
June	1.00	1.00	Null	Null	Null	Null	Null	Null	0.00	0.00	Null	Null
July	1.00	1.00	Null	Null	Null	Null	Null	Null	0.00	0.00	Null	Null
August	1.00	1.00	Null	Null	Null	Null	Null	Null	0.00	0.00	Null	Null
September	1.00	1.00	Null	Null	Null	Null	Null	Null	0.00	0.00	Null	Null
October	1.00	1.00	Null	Null	Null	Null	Null	Null	0.00	0.00	Null	Null
November	1.00	1.00	Null	Null	Null	Null	Null	Null	0.00	0.00	Null	Null
December	0.83	0.90	0.67	0.00	0.00	0.00	1.00	Null	0.07	0.00	0.00	Null

REMA: Red Estatal de Monitoreo Atmosférico (State Ambient Air Monitoring Network); CAMS: Copernicus Atmospheric Monitoring Service; Null = null value; ACCURACY: accuracy; BIAS: bias score; POD: probability of detection; FAR: false alarm rate; POFD: probability of false detection; SR: success ratio.

Table SVI**.** Comparison of dichotomous statistics of REMA and CAMS persistence air and health indices adjusted by ratio for $PM_{2.5}$ at the Ninfas station.

	Dichotomous statistics, Ninfas station $PM_{2.5}$									
	TS		ETS		HK		HSS		ORSS	
Month	REMA	CAMS	REMA	CAMS	REMA	CAMS	REMA	CAMS	REMA	CAMS
January	0.50	0.00	0.48	–0.05	0.97	–0.17	0.65	–0.10	1.00	–1.00
February	Null	0.00	Null	–0.06	Null	–0.35	Null	–0.13	Null	–1.00
March	0.17	0.00	0.11	–0.06	0.17	–0.31	0.19	–0.12	0.60	–1.00
April	0.00	0.00	–0.02	–0.03	–0.04	–0.28	–0.04	–0.06	–1.00	–1.00
May	Null	0.00	Null	0.00	Null	Null	Null	0.00	Null	Null
June	Null	Null	Null	Null	Null	Null	Null	Null	Null	Null
July	Null	Null	Null	Null	Null	Null	Null	Null	Null	Null
August	Null	Null	Null	Null	Null	Null	Null	Null	Null	Null
September	Null	Null	Null	Null	Null	Null	Null	Null	Null	Null
October	Null	Null	Null	Null	Null	Null	Null	Null	Null	Null
November	Null	Null	Null	Null	Null	Null	Null	Null	Null	Null
December	0.00	0.00	–0.04	0.00	–0.07	0.00	–0.09	0.00	–1.00	Null

REMA: Red Estatal de Monitoreo Atmosférico (State Ambient Air Monitoring Network); CAMS: Copernicus Atmospheric Monitoring Service; Null = null value; TS: threat score; ETS: equitable threat score**;** HSS: Heidke skill score; ORSS: odds ratio skill score.

Table SVII**.** Comparison of dichotomous statistics of REMA and CAMS persistence air and health indices adjusted by ratio for $PM_{2.5}$ at the UTP station.

	Dichotomous statistics, UTP station $PM_{2.5}$											
	ACCURACY		BIAS		POD		FAR		POFD		SR	
Month	REMA	CAMS	REMA	CAMS	REMA	CAMS	REMA	CAMS	REMA	CAMS	REMA	CAMS
January	0.90	0.87	2.00	1.00	0.00	0.00	1.00	1.00	0.07	0.07	0.00	0.00
February	0.93	0.89	1.00	0.50	0.00	0.00	1.00	1.00	0.04	0.04	0.00	0.00
March	0.83	0.84	0.67	1.50	0.00	0.00	1.00	1.00	0.07	0.10	0.00	0.00
April	0.86	0.63	1.00	5.50	0.00	0.50	1.00	0.91	0.07	0.36	0.00	0.09
May	1.00	0.68	Null	Null	Null	Null	Null	1.00	0.00	0.32	Null	0.00
June	0.93	0.97	1.00	0.00	0.00	0.00	1.00	Null	0.04	0.00	0.00	Null
July	0.93	0.94	1.00	1.00	0.00	0.00	1.00	1.00	0.03	0.03	0.00	0.00
August	1.00	1.00	Null	Null	Null	Null	Null	Null	0.00	0.00	Null	Null
September	0.93	0.97	1.00	0.00	0.00	0.00	1.00	Null	0.04	0.00	0.00	Null
October	1.00	1.00	Null	Null	Null	Null	Null	Null	0.00	0.00	Null	Null
November	1.00	1.00	Null	Null	Null	Null	Null	Null	0.00	0.00	Null	Null
December	0.90	0.81	0.50	2.00	0.00	0.00	1.00	1.00	0.04	0.14	0.00	0.00

REMA: Red Estatal de Monitoreo Atmosférico (State Ambient Air Monitoring Network); CAMS: Copernicus Atmospheric Monitoring Service; Null = null value; ACCURACY: accuracy; BIAS: bias score; POD: probability of detection; FAR: false alarm rate; POFD: probability of false detection; SR: success ratio.

Table SVIII**.** Comparison of dichotomous statistics of REMA and CAMS persistence air and health indices adjusted by ratio for $PM_{2.5}$ at the UTP station.

	Dichotomous statistics, UTP station $PM_{2.5}$									
	TS		ETS		HK		HSS		ORSS	
Month	REMA	CAMS	REMA	CAMS	REMA	CAMS	REMA	CAMS	REMA	CAMS
January	0.00	0.00	–0.02	–0.03	–0.07	–0.07	–0.05	–0.07	–1.00	–1.00
February	0.00	0.00	–0.02	–0.02	–0.04	–0.04	–0.04	–0.05	–1.00	–1.00
March	0.00	0.00	–0.04	–0.04	–0.07	–0.10	–0.09	–0.08	–1.00	–1.00
April	0.00	0.08	–0.04	0.02	–0.07	0.14	–0.07	0.05	–1.00	0.29
May	Null	0.00	Null	0.00	Null	Null	Null	0.00	Null	Null
June	0.00	0.00	–0.02	0.00	–0.04	0.00	–0.04	0.00	–1.00	Null
July	0.00	0.00	–0.02	–0.02	–0.03	–0.03	–0.03	–0.03	–1.00	–1.00
August	Null	Null	Null	Null	Null	Null	Null	Null	Null	Null
September	0.00	0.00	–0.02	0.00	–0.04	0.00	–0.04	0.00	–1.00	Null
October	Null	Null	Null	Null	Null	Null	Null	Null	Null	Null
November	Null	Null	Null	Null	Null	Null	Null	Null	Null	Null
December	0.00	0.00	–0.02	–0.04	–0.04	–0.14	–0.05	–0.09	–1.00	–1.00

REMA: Red Estatal de Monitoreo Atmosférico (State Ambient Air Monitoring Network); CAMS: Copernicus Atmospheric Monitoring Service; Null = null value; TS: threat score; ETS: equitable threat score**;** HSS: Heidke skill score; ORSS: odds ratio skill score.

Table SIX. Comparison of dichotomous statistics of REMA and CAMS persistence air and health indices adjusted by ratio for PM_{10} at the Agua Santa station.

	Dichotomous statistics, Agua Santa station PM_{10}											
	ACCURACY		BIAS		POD		FAR		POFD		SR	
Month	REMA	CAMS	REMA	CAMS	REMA	CAMS	REMA	CAMS	REMA	CAMS	REMA	CAMS
January	1.00	1.00	Null	Null	Null	Null	Null	Null	0.00	0.00	Null	Null
February	0.96	0.57	0.92	1.17	0.92	0.58	0.00	0.50	0.00	0.44	1.00	0.50
March	0.80	0.87	1.00	0.85	0.88	0.85	0.12	0.00	0.60	0.00	0.88	1.00
April	0.86	0.80	1.00	0.93	0.93	0.86	0.07	0.08	1.00	1.00	0.93	0.92
May	0.53	0.52	1.00	1.45	0.30	0.55	0.70	0.63	0.35	0.50	0.30	0.38
June	0.93	0.87	1.00	3.00	0.00	0.00	1.00	1.00	0.04	0.10	0.00	0.00
July	0.93	0.94	1.00	0.00	0.50	0.00	0.50	Null	0.04	0.00	0.50	Null
August	1.00	1.00	Null	Null	Null	Null	Null	Null	0.00	0.00	Null	Null
September	1.00	1.00	Null	Null	Null	Null	Null	Null	0.00	0.00	Null	Null
October	0.90	0.90	0.67	0.00	0.33	0.00	0.50	Null	0.04	0.00	0.50	Null
November	0.79	0.67	1.00	1.67	0.67	0.78	0.33	0.53	0.15	0.38	0.67	0.47
December	0.83	0.74	0.96	1.17	0.88	0.92	0.09	0.21	0.33	0.86	0.91	0.79

REMA: Red Estatal de Monitoreo Atmosférico (State Ambient Air Monitoring Network); CAMS: Copernicus Atmospheric Monitoring Service; Null = null value; ACCURACY: accuracy; BIAS: bias score; POD: probability of detection; FAR: false alarm rate; POFD: probability of false detection; SR: success ratio.

Table SX. Comparison of dichotomous statistics of REMA and CAMS persistence air and health indices adjusted by ratio for PM_{10} at the Agua Santa station.

	Dichotomous statistics, Agua Santa station PM_{10}									
	TS		ETS		HK		HSS		ORSS	
Month	REMA	CAMS	REMA	CAMS	REMA	CAMS	REMA	CAMS	REMA	CAMS
January	Null	Null	Null	Null	Null	Null	Null	Null	Null	Null
February	0.92	0.37	0.86	0.08	0.92	0.15	0.92	0.14	1.00	0.29
March	0.79	0.85	0.16	0.47	0.28	0.85	0.28	0.64	0.66	1.00
April	0.86	0.80	–0.04	–0.05	–0.07	–0.14	–0.07	–0.10	–1.00	–1.00
May	0.18	0.29	–0.02	0.02	–0.05	0.05	–0.05	0.04	–0.11	0.09
June	0.00	0.00	–0.02	–0.03	–0.04	–0.10	–0.04	–0.05	–1.00	–1.00
July	0.33	0.00	0.30	0.00	0.46	0.00	0.46	0.00	0.93	Null
August	Null	Null	Null	Null	Null	Null	Null	Null	Null	Null
September	Null	Null	Null	Null	Null	Null	Null	Null	Null	Null
October	0.25	0.00	0.21	0.00	0.30	0.00	0.35	0.00	0.86	Null
November	0.50	0.41	0.35	0.20	0.52	0.40	0.52	0.33	0.84	0.70
December	0.81	0.73	0.34	0.04	0.54	0.06	0.51	0.07	0.87	0.29

REMA: Red Estatal de Monitoreo Atmosférico (State Ambient Air Monitoring Network); CAMS: Copernicus Atmospheric Monitoring Service; Null = null value; TS: threat score; ETS: equitable threat score**;** HSS: Heidke skill score; ORSS: odds ratio skill score.

Table SXI. Comparison of dichotomous statistics of REMA and CAMS persistence air and health indices adjusted by ratio for PM_{10} at the BINE station.

	Dichotomous statistics, BINE station PM_{10}											
	ACCURACY		BIAS		POD		FAR		POFD		SR	
Month	REMA	CAMS	REMA	CAMS	REMA	CAMS	REMA	CAMS	REMA	CAMS	REMA	CAMS
January	0.70	0.65	0.86	2.29	0.29	0.86	0.67	0.63	0.17	0.42	0.33	0.38
February	0.59	0.50	0.95	1.11	0.68	0.68	0.28	0.38	0.63	0.89	0.72	0.62
March	0.57	0.58	1.06	1.05	0.67	0.68	0.37	0.35	0.58	0.58	0.63	0.65
April	0.48	0.67	0.95	1.11	0.58	0.79	0.39	0.29	0.70	0.55	0.61	0.71
May	0.87	0.61	1.00	3.67	0.33	0.33	0.67	0.91	0.07	0.36	0.33	0.09
June	0.93	0.93	1.00	1.00	0.00	0.00	1.00	1.00	0.04	0.03	0.00	0.00
July	0.73	0.45	1.00	1.43	0.43	0.00	0.57	1.00	0.17	0.42	0.43	0.00
August	1.00	0.90	Null	Null	Null	Null	Null	1.00	0.00	0.10	Null	0.00
September	0.86	0.87	1.00	1.00	0.00	0.00	1.00	1.00	0.07	0.07	0.00	0.00
October	0.93	0.84	1.00	1.50	0.50	0.00	0.50	1.00	0.04	0.10	0.50	0.00
November	0.79	0.83	1.00	1.60	0.40	0.80	0.60	0.50	0.13	0.16	0.40	0.50
December	0.77	0.87	0.95	1.21	0.79	1.00	0.17	0.17	0.27	0.33	0.83	0.83

REMA: Red Estatal de Monitoreo Atmosférico (State Ambient Air Monitoring Network); CAMS: Copernicus Atmospheric Monitoring Service; Null = null value; ACCURACY: accuracy; BIAS: bias score; POD: probability of detection; FAR: false alarm rate; POFD: probability of false detection; SR: success ratio.

Table SXII. Comparison of dichotomous statistics of REMA and CAMS persistence air and health indices adjusted by ratio for PM_{10} at the BINE station.

	Dichotomous statistics, BINE station PM_{10}									
	TS		ETS		HK		HSS		ORSS	
Month	REMA	CAMS	REMA	CAMS	REMA	CAMS	REMA	CAMS	REMA	CAMS
January	0.18	0.35	0.06	0.18	0.11	0.44	0.12	0.30	0.31	0.79
February	0.54	0.48	0.03	–0.10	0.06	–0.20	0.06	–0.22	0.13	–0.57
March	0.48	0.50	0.04	0.05	0.08	0.10	0.08	0.10	0.18	0.21
April	0.42	0.60	–0.06	0.15	–0.12	0.24	–0.12	0.25	–0.26	0.52
May	0.20	0.08	0.15	–0.01	0.26	–0.02	0.26	–0.01	0.72	–0.05
June	0.00	0.00	–0.02	–0.02	–0.04	–0.03	–0.04	–0.03	–1.00	–1.00
July	0.27	0.00	0.15	–0.15	0.25	–0.42	0.25	–0.36	0.56	–1.00
August	Null	0.00	Null	0.00	Null	Null	Null	0.00	Null	Null
September	0.00	0.00	–0.04	–0.03	–0.07	–0.07	–0.07	–0.07	–1.00	–1.00
October	0.33	0.00	0.30	–0.04	0.46	–0.10	0.46	–0.08	0.93	–1.00
November	0.25	0.44	0.16	0.35	0.28	0.64	0.28	0.52	0.65	0.91
December	0.68	0.83	0.34	0.55	0.52	0.67	0.51	0.71	0.82	1.00

REMA: Red Estatal de Monitoreo Atmosférico (State Ambient Air Monitoring Network); CAMS: Copernicus Atmospheric Monitoring Service; Null = null value; TS: threat score; ETS: equitable threat score; HSS: Heidke skill score; ORSS: odds ratio skill score.

Table SXIII. Comparison of dichotomous statistics of REMA and CAMS persistence air and health indices adjusted by ratio for PM_{10} at the Ninfas station.

	Dichotomous statistics, Ninfas station PM_{10}											
	ACCURACY		BIAS		POD		FAR		POFD		SR	
Month	REMA	CAMS	REMA	CAMS	REMA	CAMS	REMA	CAMS	REMA	CAMS	REMA	CAMS
January	0.67	0.61	1.00	1.20	0.74	0.80	0.26	0.33	0.45	0.73	0.74	0.67
February	0.93	0.82	1.00	1.04	0.96	0.92	0.04	0.12	0.33	1.00	0.96	0.88
March	0.80	0.74	1.00	0.92	0.88	0.81	0.12	0.13	0.60	0.60	0.88	0.88
April	0.93	0.87	1.00	0.93	0.96	0.90	0.04	0.04	1.00	1.00	0.96	0.96
May	0.80	0.61	1.00	1.67	0.50	0.33	0.50	0.80	0.13	0.32	0.50	0.20
June	0.93	0.90	1.00	0.50	0.50	0.00	0.50	1.00	0.04	0.04	0.50	0.00
July	0.63	0.61	0.90	1.40	0.40	0.60	0.56	0.57	0.25	0.38	0.44	0.43
August	0.93	0.84	1.00	4.00	0.00	0.00	1.00	1.00	0.03	0.13	0.00	0.00
September	0.93	0.97	1.00	0.00	0.00	0.00	1.00	Null	0.04	0.00	0.00	Null
October	0.93	0.97	1.00	0.00	0.00	0.00	1.00	Null	0.03	0.00	0.00	Null
November	0.72	0.70	1.00	0.80	0.20	0.00	0.80	1.00	0.17	0.16	0.20	0.00
December	0.70	0.65	0.95	1.14	0.77	0.82	0.19	0.28	0.50	0.78	0.81	0.72

REMA: Red Estatal de Monitoreo Atmosférico (State Ambient Air Monitoring Network); CAMS: Copernicus Atmospheric Monitoring Service; Null = null value; ACCURACY: accuracy; BIAS: bias score; POD: probability of detection; FAR: false alarm rate; POFD: probability of false detection; SR: success ratio.

Table SXIV. Comparison of dichotomous statistics of REMA and CAMS persistence air and health indices adjusted by ratio for PM_{10} at the Ninfas station.

	Dichotomous statistics, Ninfas station PM_{10}									
	TS		ETS		HK		HSS		ORSS	
Month	REMA	CAMS	REMA	CAMS	REMA	CAMS	REMA	CAMS	REMA	CAMS
January	0.58	0.57	0.16	0.04	0.28	0.07	0.28	0.08	0.54	0.20
February	0.92	0.82	0.45	–0.04	0.63	–0.08	0.63	–0.09	0.96	–1.00
March	0.79	0.72	0.16	0.10	0.28	0.21	0.28	0.18	0.66	0.47
April	0.93	0.87	–0.02	–0.03	–0.04	–0.10	–0.04	–0.05	–1.00	–1.00
May	0.33	0.14	0.23	0.01	0.38	0.01	0.38	0.01	0.75	0.03
June	0.33	0.00	0.30	–0.02	0.46	–0.04	0.46	–0.05	0.93	–1.00
July	0.27	0.33	0.08	0.11	0.15	0.22	0.15	0.20	0.33	0.42
August	0.00	0.00	–0.02	–0.03	–0.03	–0.13	–0.03	–0.05	–1.00	–1.00
September	0.00	0.00	–0.02	0.00	–0.04	0.00	–0.04	0.00	–1.00	Null
October	0.00	0.00	–0.02	0.00	–0.03	0.00	–0.03	0.00	–1.00	Null
November	0.11	0.00	0.02	–0.08	0.03	–0.16	0.03	–0.17	0.11	–1.00
December	0.65	0.62	0.15	0.02	0.27	0.04	0.26	0.04	0.55	0.13

REMA: Red Estatal de Monitoreo Atmosférico (State Ambient Air Monitoring Network); CAMS: Copernicus Atmospheric Monitoring Service; Null = null value; TS: threat score; ETS: equitable threat score**;** HSS: Heidke skill score; ORSS: odds ratio skill score.

Table SXV. Comparison of dichotomous statistics of REMA and CAMS persistence air and health indices adjusted by ratio for PM_{10} at the UTP station.

	Dichotomous statistics, UTP station PM_{10}											
	ACCURACY		BIAS		POD		FAR		POFD		SR	
Month	REMA	CAMS	REMA	CAMS	REMA	CAMS	REMA	CAMS	REMA	CAMS	REMA	CAMS
January	0.87	0.65	1.00	1.13	0.91	0.83	0.09	0.27	0.25	0.88	0.91	0.73
February	0.93	0.75	1.00	1.04	0.96	0.88	0.04	0.16	0.25	1.00	0.96	0.84
March	0.80	0.74	1.00	0.93	0.88	0.81	0.12	0.12	0.75	0.75	0.88	0.88
April	0.72	0.77	1.00	1.04	0.83	0.88	0.17	0.16	0.67	0.67	0.83	0.84
May	0.57	0.61	0.94	1.12	0.59	0.71	0.38	0.37	0.46	0.50	0.63	0.63
June	0.79	0.87	1.00	0.00	0.25	0.00	0.75	Null	0.12	0.00	0.25	Null
July	0.83	0.45	0.93	0.80	0.80	0.33	0.14	0.58	0.13	0.44	0.86	0.42
August	0.97	0.74	1.33	1.00	1.00	0.00	0.25	1.00	0.04	0.15	0.75	0.00
September	0.93	0.70	1.00	0.80	0.80	0.00	0.20	1.00	0.04	0.16	0.80	0.00
October	0.93	0.97	1.00	0.00	0.00	0.00	1.00	Null	0.03	0.00	0.00	Null
November	0.66	0.47	1.00	0.78	0.44	0.00	0.56	1.00	0.25	0.33	0.44	0.00
December	0.80	0.65	1.00	1.04	0.87	0.79	0.13	0.24	0.43	0.86	0.87	0.76

REMA: Red Estatal de Monitoreo Atmosférico (State Ambient Air Monitoring Network); CAMS: Copernicus Atmospheric Monitoring Service; Null = null value; ACCURACY: accuracy; BIAS: bias score; POD: probability of detection; FAR: false alarm rate; POFD: probability of false detection; SR: success ratio.

Table SXVI. Comparison of dichotomous statistics of REMA and CAMS persistence air and health indices adjusted by ratio for PM_{10} at the UTP station.

	Dichotomous statistics, UTP station PM_{10}									
	TS		ETS		HK		HSS		ORSS	
Month	REMA	CAMS	REMA	CAMS	REMA	CAMS	REMA	CAMS	REMA	CAMS
January	0.83	0.63	0.49	–0.03	0.66	–0.05	0.66	–0.06	0.94	–0.19
February	0.92	0.75	0.55	–0.07	0.71	–0.13	0.71	–0.14	0.97	–1.00
March	0.79	0.73	0.07	0.03	0.13	0.06	0.13	0.05	0.44	0.19
April	0.70	0.75	0.09	0.13	0.16	0.21	0.16	0.22	0.41	0.56
May	0.43	0.50	0.07	0.12	0.13	0.21	0.13	0.21	0.25	0.41
June	0.14	0.00	0.07	0.00	0.13	0.00	0.13	0.00	0.42	Null
July	0.71	0.23	0.50	–0.05	0.67	–0.10	0.67	–0.10	0.93	–0.22
August	0.75	0.00	0.72	–0.07	0.96	–0.15	0.84	–0.15	1.00	–1.00
September	0.67	0.00	0.61	–0.08	0.76	–0.16	0.76	–0.17	0.98	–1.00
October	0.00	0.00	–0.02	0.00	–0.03	0.00	–0.03	0.00	–1.00	Null
November	0.29	0.00	0.11	–0.15	0.19	–0.33	0.19	–0.36	0.41	–1.00
December	0.77	0.63	0.28	–0.03	0.44	–0.07	0.44	–0.07	0.80	–0.22

REMA: Red Estatal de Monitoreo Atmosférico (State Ambient Air Monitoring Network); CAMS: Copernicus Atmospheric Monitoring Service; Null = null value; TS: threat score; ETS: equitable threat score; HSS: Heidke skill score; ORSS: odds ratio skill score.

Table SXVII. Comparison of dichotomous statistics of REMA and CAMS persistence air and health indices adjusted by ratio for PM_{10} at the Velódromo station.

	Dichotomous statistics, Velódromo station PM_{10}											
	ACCURACY		BIAS		POD		FAR		POFD		SR	
Month	REMA	CAMS	REMA	CAMS	REMA	CAMS	REMA	CAMS	REMA	CAMS	REMA	CAMS
January	0.70	0.58	0.83	2.50	0.17	0.67	0.80	0.73	0.17	0.44	0.20	0.27
February	0.78	0.75	1.00	0.44	0.67	0.33	0.33	0.25	0.17	0.05	0.67	0.75
March	0.93	0.58	1.00	0.58	0.92	0.25	0.08	0.57	0.06	0.21	0.92	0.43
April	0.93	0.97	1.00	0.00	0.00	0.00	1.00	Null	0.04	0.00	0.00	Null
May	1.00	1.00	Null	Null	Null	Null	Null	Null	0.00	0.00	Null	Null
June	1.00	1.00	Null	Null	Null	Null	Null	Null	0.00	0.00	Null	Null
July	1.00	1.00	Null	Null	Null	Null	Null	Null	0.00	0.00	Null	Null
August	1.00	1.00	Null	Null	Null	Null	Null	Null	0.00	0.00	Null	Null
September	1.00	1.00	Null	Null	Null	Null	Null	Null	0.00	0.00	Null	Null
October	1.00	1.00	Null	Null	Null	Null	Null	Null	0.00	0.00	Null	Null
November	1.00	1.00	Null	Null	Null	Null	Null	Null	0.00	0.00	Null	Null
December	1.00	1.00	Null	Null	Null	Null	Null	Null	0.00	0.00	Null	Null

REMA: Red Estatal de Monitoreo Atmosférico (State Ambient Air Monitoring Network); CAMS: Copernicus Atmospheric Monitoring Service; Null = null value; ACCURACY: accuracy; BIAS: bias score; POD: probability of detection; FAR: false alarm rate; POFD: probability of false detection; SR: success ratio.

Table SXVIII. Comparison of dichotomous statistics of REMA and CAMS persistence air and health indices adjusted by ratio for PM_{10} at the Velódromo station.

	Dichotomous statistics, Velódromo station PM_{10}									
	TS		ETS		HK		HSS		ORSS	
Month	REMA	CAMS	REMA	CAMS	REMA	CAMS	REMA	CAMS	REMA	CAMS
January	0.10	0.24	0.00	0.08	0.00	0.23	0.00	0.14	0.00	0.44
February	0.50	0.30	0.33	0.20	0.50	0.28	0.50	0.33	0.82	0.80
March	0.85	0.19	0.76	0.02	0.86	0.04	0.86	0.04	0.99	0.11
April	0.00	0.00	–0.02	0.00	–0.04	0.00	–0.04	0.00	–1.00	Null
May	Null	Null	Null	Null	Null	Null	Null	Null	Null	Null
June	Null	Null	Null	Null	Null	Null	Null	Null	Null	Null
July	Null	Null	Null	Null	Null	Null	Null	Null	Null	Null
August	Null	Null	Null	Null	Null	Null	Null	Null	Null	Null
September	Null	Null	Null	Null	Null	Null	Null	Null	Null	Null
October	Null	Null	Null	Null	Null	Null	Null	Null	Null	Null
November	Null	Null	Null	Null	Null	Null	Null	Null	Null	Null
December	Null	Null	Null	Null	Null	Null	Null	Null	Null	Null

REMA: Red Estatal de Monitoreo Atmosférico (State Ambient Air Monitoring Network); CAMS: Copernicus Atmospheric Monitoring Service; Null = null value; TS: threat score; ETS: equitable threat score**;** HSS: Heidke skill score; ORSS: odds ratio skill score.